Higgs vacuum stability in Standard Model extensions

Ashley C. Arsenault

A Thesis

in

The Department

of

Physics

Presented in Partial Fulfillment of the Requirements

for the Degree of

Master of Science (Physics) at

Concordia University

Montréal, Québec, Canada

July 2017

Concordia University

School of Graduate Studies

This is to certify that the thesis prepared

By: **Ashley C. Arsenault**

Entitled: **Higgs vacuum stability in Standard Model extensions**

and submitted in partial fulfillment of the requirements for the degree of

Master of Science (Physics)

complies with the regulations of this University and meets the accepted standards with respect to originality and quality.

Signed by the Final Examining Committee:

_____ Chair
Dr. Alexandre Champagne

_____ Examiner
Dr. Panagiotis Vasilopoulos

_____ Supervisor
Dr. Mariana Frank

Approved by   _____

Alexandre Champagne, Chair
Department of Physics

_____ 2017   _____

André Roy, Dean
Faculty of Arts & Science

Abstract

Higgs vacuum stability in Standard Model extensions

Ashley C. Arsenault

After 40 years of searching, the Higgs boson was finally found at CERN's Large Hadron Collider in 2012 and weighed in at 125 GeV. However, this small mass gives rise to a vacuum stability problem, namely that the Standard Model Higgs quartic self-coupling becomes negative below the Planck scale, necessitating new physics beyond the Standard Model.

In this thesis, we study four minimal extensions of the Standard Model which solve the Higgs vacuum stability problem by adding a second Higgs-like scalar boson. In addition to the new scalar boson, we study the effects of adding new fermion singlets and doublets. It is shown that while new fermion generations only decrease the Higgs quartic coupling at high energies—only exacerbating the problem—the addition of a new Higgs-like scalar provides a positive contribution which is enough to overcome the vacuum stability limit.

We consider four Standard Model extensions containing different combinations of new fermions with this extended Higgs sector, and identify the allowed masses and mass mixing angles of these hypothetical particles that satisfy the vacuum stability condition. The allowed masses surround the 1 TeV range approximately, explaining why such particles have not yet been found.

Acknowledgments

First and foremost, I would like to sincerely thank my thesis advisor, Dr. Mariana Frank of the Physics Department at Concordia University. Not only has she been a great inspiration as an academic and a researcher, but as a well-rounded mentor whose passion for student learning is both refreshing and infectious.

I would also like to take the time to thank my examining committee members, Dr. Alexandre Champagne and Dr. Panagiotis Vasilopoulos, for their careful review of my first draft and their insightful feedback and suggestions that could only come from such brilliant researchers with great attention to detail.

A warm thanks also goes out to the Physics Department faculty members as well as my fellow students; especially Jack, who has always been eager to offer a helping hand, encouragement, and friendship.

Finally, I thank my friends and family for their continued love and support; Mom, Dad, Matthew, Renée, Zoey, Chase, Zuzia, Gwenn, and Nasser, to name only a few. I owe you all my gratitude for keeping me motivated and encouraged.

Pass on what you have learned.

YODA

Contribution of the Author

The original research work contained in this thesis is presented in Chapter 6 and has been conducted in collaboration with Prof. Mariana Frank.

In Chapter 6, some of the analytical and all computational calculations which led to the final results of the research was conducted by the author in partial fulfillment of the requirements for the Master of Science degree in the Department of Physics at Concordia University, Montreal, Quebec.

As well, the production of the graphs in Chapter 6, along with Figures 5.1, 5.2, 5.7(a) and 5.7(c), was conducted by the author.

Contents

List of Figures

Chapter 1

Introduction

The field of particle physics is a very dynamic area of research, with over fifty Nobel Prizes awarded in the field to date. The term "particle physics" is interchangeable with "high energy physics", because many elementary particles do not occur naturally, but rather are created only during high energy collisions with other particles, as can be detected by particle accelerators. For this reason, as technological advances allow us to reach higher and higher energies, our knowledge in this field is expanding all the time.

The idea that all matter is made up of elementary particles has been in existence since 460 BC. Aristotle, along with the majority of Greek philosophers at the time, believed that all matter could be divided infinitely without changing its properties. However, Democritus postulated that there reached a point when matter could no longer be broken up any further, and that all matter was made up of these small indivisible fragments called atoms. In principle, he believed that there were an infinite number of elementary atoms: iron was made of iron atoms, clay was made of clay atoms, and cheese was made of cheese atoms. Later, Hindu philosophers proposed that atoms came in only four flavours: earth, air, fire, and water. However, this idea of the atom was purely intuitive and had no scientific credibility for many years.

In fact, it was not until 1803 that John Dalton, an English chemist, observed atoms while experimenting with gases. Dalton's atomic model is often referred to as the "billiard ball" model, because he assumed that atoms were merely hard spheres that could not be divided into smaller pieces. He postulated that there exists a different atom for each element of the periodic table, and formulated a theory which states that all matter is made of atoms, that atoms are indivisible and indestructible, that all atoms of a given element are identical, and that compounds are made from combinations of these atoms. Dalton's atomic theory quickly became well-respected in chemistry and even today, while modern atomic theory is much more involved, the essence of his theory still remains valid.

In 1897, J.J. Thomson showed that cathode rays were composed of electrically charged particles, which he called corpuscles (now known as electrons). He calculated that these electrons must have a mass a thousand times lighter than a hydrogen atom, which was the lightest known atom at the time. Thomson knew that the atom had an overall neutral charge, and concluded that atoms were actually positively charged cores that contained negatively charged electrons within them. This model of the atom is known as the "plum pudding" model, because the electrons were thought to be floating freely throughout the positively charged core, like plums scattered throughout plum pudding.

In 1909, Ernest Rutherford, a student of Thomson's, designed an experiment in which alpha particles—small positively charged particles which remained mostly a mystery at the time, but are now understood to be the helium nucleus—were fired at a piece of foil, with a detector screen placed in a circular fashion around it. Assuming the plum pudding model was correct and that the charges were scattered throughout the gold atoms, the alpha radiation should have passed directly through the gold foil as the charge was thought to be scattered sparsely throughout the atom. However, he observed that while most alpha particles did pass directly through the foil, several were also scattered away from the foil at various angles. This proved to Rutherford that atoms had to possess a heavy, positively charged nucleus (i.e. the positive charge was concentrated in a much smaller volume than predicted by Thomson's model) in order to produce a force great enough to

repel the heavy, positively charged alpha particles in such a fashion. This solar system model with electrons orbiting the nucleus is known as the Rutherford model. Rutherford later bombarded nitrogen with alpha particles, producing hydrogen ions, which he identified as fundamental particles that he called protons.

In 1913, Neils Bohr furthered Rutherford's work and presented us with the Bohr model. He pointed out that the electron's centripetal force and Coulomb force must be equal in order to hold the electron in its stable orbit about the nucleus, and derived the discrete energy values allowed, along with their corresponding orbital distances. He surmised that electrons were only allowed to jump from one orbital to a higher or lower orbital by absorbing or emitting photons, respectively.

The modern quantum mechanical atomic model was established in 1927 by theoretical physicist Werner Heisenberg. According to Heisenberg's uncertainty principle, it is impossible to know both a particle's position and momentum simultaneously—the more precisely the position is determined, the less precisely its momentum can be known, and vice versa. This is due to the wavelike nature of matter. As a result of this formulation, rather than traveling in orbits, electrons exist as "clouds" within these orbitals, the clouds defining regions of space with a high probability of containing the electron.
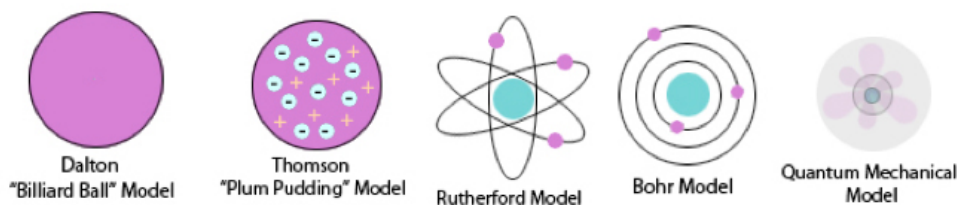
Figure 1.1: A timeline of the atomic model, beginning with Dalton's "billiard ball" model and ending with the modern quantum mechanical model.

As we now know, particles are not only responsible for matter, but for forces as well. This discovery came surprisingly early in 1905 when Albert Einstein cleverly predicted the existence of the photon. He surmised that electromagnetic radiation was in fact particulate and that we live in a quantum universe, built from discrete chunks of matter and energy.

Also in 1905, he published his idea of mass-energy equivalence, suggesting that matter is simply a form of energy. In 1909, he showed that photons have momentum and energy and established the concept of wave-particle duality. Later in 1923, this photon momentum was observed experimentally by Arthur Compton [1].

Later, in 1927, Paul Dirac formulated quantum electrodynamics [2], which was essentially the first quantum field theory, describing the electromagnetic force in terms of fundamental particle interactions involving the photon. This gave birth to the modern idea that elementary particle fields are responsible for fundamental forces as well as matter.

In the early 1960s, Sheldon Glashow, Abdus Salam and Steven Weinberg furthered the early foundations of the Standard Model by merging electromagnetic and weak interactions, giving rise to what we now call electroweak theory [3]. This was the early foundation of the Standard Model, or SM, upon which other interactions built upon.

In 1964, Peter Higgs theorized the existence of a field responsible for giving particles mass. This field bears his name, and the excitement of this field gives rise to the Higgs boson [4]. The Higgs mechanism was then bridged into electroweak theory in 1967 by Steven Weinberg [5]. Finally, the last known piece of the Standard Model, known as the theory of quantum chromodynamics (QCD), which describes the strong force in terms of elementary particle interactions, was fine-tuned around 1973 and had several contributors [6, 7].

It was only recently, in 2012, that the Higgs boson was discovered experimentally at CERN's Large Hadron Collider, confirming at last the long-standing Higgs theory [8, 9]. However, the observed mass of the Higgs boson, at 125 GeV, surprised physicists, as it violates Higgs vacuum stability [10, 11, 12], which will be explained in greater detail later in this thesis. The result of this unexpectedly low mass is that either the Standard Model must be incorrect or flawed in some way, or at the very least, that new physics must exist at higher energies.

Minimal extensions of the Standard Model which stabilize the Higgs vacuum are the most

common theories which attempt to solve the Higgs mass problem. The correlation between the Higgs mass and vacuum stability is highly dependent on the particles involved in bosonic interactions. For this reason, models proposing as few as one additional particle in the Standard Model are capable of stabilizing the electroweak vacuum. Supersymmetry and extra dimensions are also Higgs vacuum stabilizing candidates and they predict new particles and interactions. However, these theories have so far proven difficult to confirm experimentally. In addition, extra particles not only provide a simple solution to the vacuum stability problem, but so do they have the potential to answer other remaining questions that the Standard Model neglects, such as dark matter [13, 14, 15, 16, 17].

One simple type of extension of the Standard Model which takes care of vacuum stability is additional Higgs-like particle models, such as the two Higgs doublet model, which introduces a second, heavier, Higgs-like scalar boson [18] and the Higgs triplet model [19, 20, 21, 22]. The two-Higgs model stands by itself, but it is also sometimes studied in dark matter exploration, where the added scalar is introduced as a dark matter candidate. This model along with some variations are the focus of this thesis, the simplest of which includes an extra fermion as well as the extra scalar boson [23, 24].

Other recently explored minimal extensions include new types of particles altogether, such as the leptoquark model [25], which introduces a hypothetical boson which carries both colour and weak isospin, allowing it to exchange information between leptons and quarks. It carries a fractional electric charge and is an unstable particle which quickly decays into a lepton and quark of the same generation. Yet another model known as the seesaw mechanism explores the implications of the hypothetical existence of right-handed neutrinos which have very large mass (SM neutrinos are all left-handed and virtually massless) [22, 26, 27, 28].

In this thesis, we will study several extensions involving an extra Higgs-like scalar boson, along with different combinations of extra fermions. More specifically, we will examine the vacuum stability bound and determine the mass restraints placed on these hypothetical

particles by the vacuum stability condition. We will begin with a revision of the Standard Model and the extra scalar boson and fermion model, as presented by Ming-Lei Xiao and Jiang-Hao Yu [23], and then examine two further extensions involving new fermion generations rather than single fermions.

Chapter 2

The Standard Model

2.1 Introduction

The Standard Model of particle physics is the theory which outlines all of the known elementary particles in our universe. In addition to describing all of the known subatomic elementary particles, the Standard Model describes their interactions. These interactions come in different forms, known as three of the four fundamental forces—electromagnetic, weak, and strong interactions. The fourth fundamental force, gravity, has yet to find its place in the Standard Model, and physicists are still working diligently to merge the two.

The elementary particles contained within the Standard Model can be classified into two broad categories: fermions, the particles that make up matter; and bosons, the force-carrying particles. These two types of particles can also be identified by their spin: all fermions carry half-integer spin, while all bosons carry integer spin.

2.2 Fermions

Fermions are the fundamental building blocks of all matter. The name was chosen because these particles obey Fermi-Dirac statistics, or alternatively, the Pauli exclusion principle. The Pauli exclusion principle states that no two identical fermions can occupy the same quantum state simultaneously. Fermi-Dirac statistics describe the distribution of such particles over energy states.

For example, this property explains the distribution of an atom's electrons in their orbitals. All electrons carry a spin of 1/2, and as a result, the ground state energy can only contain two electrons—one spin up ($+1/2$), and one spin down ($-1/2$). The higher the energy state, the higher the number of possible angular momentum states, which is why the outer electron shells contain more and more electrons. Nevertheless, each electron shell can only contain two electrons for each momentum state.

In the Standard Model, fermions themselves can be broken up into two subcategories: quarks and leptons.

2.2.1 Leptons

There are a total of six leptons (or twelve, if we take into account their antimatter counterparts), made up of three generations each containing a charged lepton (of charge -1) and a very light, neutrally charged neutrino that shares its name. The first generation is made up of the electron and the electron neutrino; the second generation corresponds to the muon, which is heavier than the electron, and the muon neutrino; and the third generation contains the tau, the heaviest lepton, and the tau neutrino (see Figure 2.1).

The leptons participate in all interactions except strong interactions. However, the weak force is a very short-range interaction, so neutrinos (which have a neutral charge and thus are also unaffected by the electromagnetic force) rarely interact with anything and typically

Figure 2.1: The Standard Model.

pass right through matter undetected.

2.2.2 Quarks

Quarks, like leptons, come in six flavours divided into three successively heavier generations. However, unlike leptons, quarks have never been directly observed on their own—they are bound together by the strong force in nature, and as a result, their individual charges come in fractions of e. The up, charm, and top quarks each have a charge of $+2/3$, while the down, strange, and bottom quarks have a charge of $-1/3$.

As participants of strong interactions, quarks possess a property that we call "colour", which comes in three distinct values labeled red, green, and blue. Anti-quarks, on the other hand, come in anti-red, anti-green, and anti-blue. In order to explain the possible

groupings of quarks, we require all physical particles to be colourless. As such, we can mix three differently coloured quarks or anti-quarks together (one red, one green, and one blue—or, conversely, one anti-red, one anti-green, and one anti-blue) to form a composite particle called a baryon (examples include protons and neutrons), or we can mix one quark and one anti-quark of the same colour (red and anti-red, for example) to form mesons, such as pions and kaons. Collectively, we refer to baryons and mesons as hadrons.

2.3   Bosons

Bosons are named after Bose-Einstein statistics, which govern their distribution across discrete energy states. The number of bosons which can occupy the same state, unlike fermions, varies with temperature.

Bosons are the particles responsible for the four fundamental forces. The photon is responsible for the electromagnetic force, the gluon for the strong force, and the $W^{\pm}$ and Z bosons (three different particles carrying charges of -1, 0, and 1) for the weak force (the graviton is thought to mediate the gravitational force, but such a particle has still not yet been discovered experimentally). These four forces and their associated mediator particles are listed below in order of decreasing approximate strength, as given in a popular particle physics textbook, "Introduction to Elementary Particles," by David J. Griffiths [29]. Note that gravity is not part of the Standard Model, and we list it for comparison only.

Force	Strength	Theory	Mediator
Strong	10	Quantum Chromodynamics (QCD)	Gluon
Electromagnetic	10^{-2}	Quantum Electrodynamics (QED)	Photon
Weak	10^{-13}	Flavordynamics	W and Z
Gravitational	10^{-42}	Geometrodynamics	Graviton

2.4 Feynman diagrams

We illustrate particle interactions using Feynman diagrams, as illustrated in Figure 2.2. The vertices joining bosons with fermions or other bosons in such diagrams represent the various individual interactions. All particle interactions must involve the presence of at least one of the force-mediating bosons. However, they are often short-lived, and as a result, they are sometimes referred to as "virtual particles", which are not physical particles, but mere disturbances in the particle fields.

When making use of Feynman diagrams, it is important to note that momentum and charge must be conserved at every vertex. Furthermore, fermions always appear in pairs of the same type at any given vertex with arrows always pointing in the same direction, as illustrated above. The number of fermions entering and exiting an interaction is conserved.

2.5 The Higgs boson

It is important to understand that all fundamental particle interactions involve at least one boson, and that the four fundamental forces observed in nature (if we assume the existence of the graviton) are described by such interactions. An interaction with one or
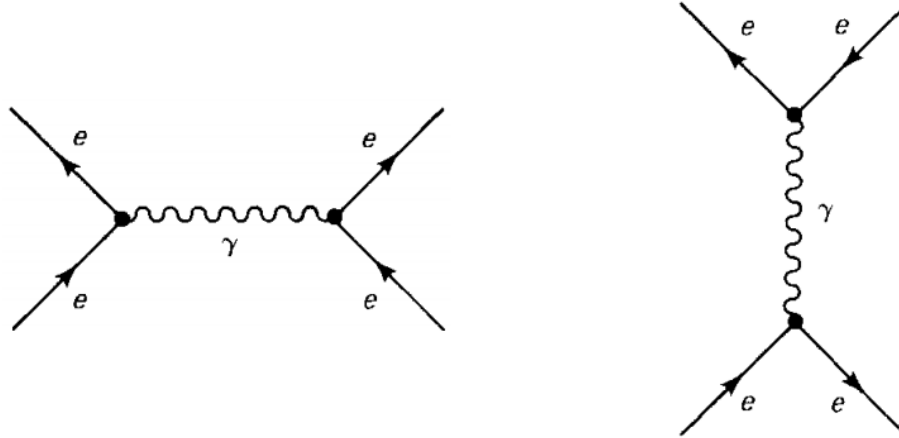
(a) Two electrons exchange a photon (the originating electron is irrelevant). This exchange of momentum allows for the electrons to repel one another.

(b) An electron and a positron annihilate one another to create a virtual photon, which then produces an electron-positron pair.

Figure 2.2: An example of two Feynman diagrams illustrating typical electromagnetic interactions. The horizontal axis represents position, while the vertical axis represents time (However, this convention is arbitrary and is reversed in many textbooks). The arrows that appear to point backwards in time represent anti-particles.

more photons gives rise to the electromagnetic force; one with W and Z bosons gives rise to the weak force; those with gluons, the strong force; and an interaction involving the hypothetical graviton would describe the gravitational force. Feynman diagrams are used to illustrate these interactions on their smallest, most fundamental scale. These diagrams often include virtual particles, which can be described simply as particles that exist within the diagram for a brief moment in time as an intermediate step—whether or not the particle physically existed as part of the process is irrelevant. Every particle interaction can then be described by an infinite number of Feynman diagrams, each one containing more virtual particles than the last. Lower-order Feynman diagrams are far more likely to occur as a physical process than those described by higher-order Feynman diagrams; however there is no way to differentiate these physical occurrences, as quantum particles must be treated in terms of probabilities. In order to accurately describe a gauge interaction, then, we must in theory account for an infinite number of Feynman diagrams. However, the higher-order diagrams become less probable and thus more negligible in mathematical considerations as

they represent higher order terms in perturbation theory.

Now, we have established that boson interactions give rise to the fundamental forces. One might then wonder why the Higgs mechanism is not considered a fifth fundamental force. We already know that fermions possess half-integer spin, while bosons possess integer spin. More specifically, the gauge bosons, which earn their name from being a direct consequence of observed symmetries, have a spin equal to 1. The component of such a particle's spin along any axis has three eigenvalues: $-\hbar$, 0, and $+\hbar$. In other words, any measurement of the spin can yield any of these three values. These 1-spin bosons are known as vector bosons. The Higgs boson, on the other hand, is the only known fundamental particle with 0-spin. The measured spin component then has only one eigenvalue: 0. Because of this, the Higgs is called a scalar boson. Our intuitive definition of force is a vector which imparts momentum, however the Higgs field is a scalar field which imparts scalar mass. Furthermore, the gauge bosons are a direct consequence of gauge symmetries and fall into place within the Standard Model naturally, while the scalar Higgs boson was inserted into the Model in order to explain electroweak symmetry breaking which allows all particles in the Standard Model to acquire mass, and which we will explore further in the next chapter. For these reasons, the Higgs is categorized alone, apart from the gauge bosons, and we do not define the Higgs mechanism as a fundamental force.

Chapter 3

Background Theory

3.1 The Higgs Mechanism

The Higgs mechanism, defined as the process which gives mass to particles in the Standard Model, is introduced in a very comprehensible manner in [30], which will be summarized here.

The need for the Higgs mechanism arises purely from our desire for symmetry in nature as physicists. To put it differently, we use the Higgs mechanism to explain why an observation does not match a recurring pattern.

We begin by studying the classical formula for potential energy. Just as in [30], let us consider a charged particle in an electric field in vacuum as an example. The potential energy of the particle is

$$U = qV, \tag{1}$$

where q is the charge of the particle and V is the potential, which is a function of the electric field $\vec{E}$. This potential energy represents the interaction of the particle with the electric field.

The potential energy of the electric field in a volume $\mathcal{V}$, on the other hand, is

$$U = \frac{\epsilon_0}{2} \int |\vec{E}|^2 d\mathcal{V}, \tag{2}$$

where ϵ_0 is the dielectric constant of the vacuum. This potential energy arises from the electric field's interaction with itself.

The total potential energy inside the volume $\mathcal{V}$ is then

$$U = qV + \frac{\epsilon_0}{2} \int |\vec{E}|^2 d\mathcal{V}. \tag{3}$$

Alternatively, we may look at the energy density,

$$u \equiv \frac{dU}{d\mathcal{V}} = \frac{d}{d\mathcal{V}} qV + \frac{\epsilon_0}{2} |\vec{E}|^2. \tag{4}$$

When studying such energy densities, we typically observe a certain symmetry. The energy density is always written as a sum of terms, each representing an interaction of some field with matter (a boson with a fermion), or of a field with a field (a boson with another boson). In our example, the first term is a product of

(1) a coupling constant, q,

(2) an operator, $\frac{d}{d\mathcal{V}}$, representing the "density" of the matter in the volume, and

(3) the potential, V, of the field.

Similarly, in the second term, we have

(1) a coupling constant, $\epsilon_0/2$, and

(2) the field, $\vec{E}$.

In general, each term contains a coupling constant which quantifies the strength of the

coupling between the two interacting objects in question, as well as an operator for each of these objects, whether it be

- $\frac{d}{d\mathcal{V}}$ (matter) and a potential Φ (field), or

- ϕ_1 (field) and ϕ_2 (another field).

However, a problem arises when we attempt to introduce special relativity, for special relativity appears to break this apparent symmetry. Allowing the particle in our example (of some mass m) to be relativistic, we must now introduce Einstein's expression for the rest energy, $E = mc^2$. The total energy density then becomes

$$u = \frac{d}{d\mathcal{V}}qV + \frac{\epsilon_0}{2}|\vec{E}|^2 + \frac{d}{d\mathcal{V}}mc^2. \tag{5}$$

The problem with this new term is obvious. It does not reflect an interaction in the same way as the first two terms. It contains the operator associated with matter, the mass m (which could function as a coupling constant just like q in the first term), and finally c^2, which is simply a universal constant. If we are to treat this term as any other energy density term, we must describe it as an interaction between the particle and some new field, which we call the Higgs field.

Let us denote the Higgs field ϕ. Since we know that fields can interact with sources as well as other fields, we can expect the Higgs field to interact with the charged particle, the electric field, as well as itself in our example. Then, taking each of these possible interactions into account and following the observed symmetry, a more general expression for the energy density is

$$u = \frac{d}{d\mathcal{V}}qV + \frac{\epsilon_0}{2}|\vec{E}|^2 + \frac{d}{d\mathcal{V}}a\Phi + g\vec{E}\phi + \kappa\phi^2, \tag{6}$$

where Φ and ϕ are the Higgs potential and field respectively, and a, g, and κ are arbitrary coupling constants.

Let us now take a step back and focus on the definition of "vacuum". Intuitively, a vacuum

16

is a space in which no matter nor field exists. For example, returning to Eq.(5), we would have $m = 0$ and $\vec{E} = 0$ in a vacuum. However, the proper definition of a vacuum in physics is not necessarily a complete lack of matter or fields, but rather the state in which the energy reaches its minimum. For example, in the above example, we define the state at which the energy density u reaches its minimum, i.e. $u = 0$, as the vacuum state. In this particular case, this corresponds to the absence of matter and fields ($m = 0$ and $\vec{E} = 0$), however in general this is not necessarily the case. Now that the proper definition of the vacuum state is established, we use this definition in conjunction with the requirement for any system to seek stability in the vacuum state (like a ball rolling to the lowest point on an uneven surface) to make the following ansatz:

$$u = \frac{d}{d\mathcal{V}}qV + \frac{\epsilon_0}{2}|\vec{E}|^2 + \frac{d}{d\mathcal{V}}a\Phi + g\vec{E}\phi - \kappa^2\phi^2 + \lambda\phi^4 \tag{7}$$

This expression of the energy density is identical to the previous one, except that we have forced the Higgs self-coupling constant to be negative and added an extra higher order term, $|\phi|^4$. These higher order terms may be interpreted as combinations of the usual second-order terms, describing more complex higher order interactions.

This ansatz is made because the vacuum state (energy minimum) occurs at a nonzero value of ϕ. Near the origin, the negative term proportional to ϕ^2 dominates, and the potential is negative. However, as $\langle\phi\rangle$ increases, the term proportional to ϕ^4 dominates and causes the potential to increase, creating a local minimum at some nonzero value of $\langle\phi\rangle$. This potential, known as the Higgs potential, is illustrated in Figure 3.1.

We are interested in the vacuum state of the energy function presented in Eq.(7) because this represents the natural state of our universe—we understand that any system prefers to occupy its ground state. The ansatz presented above describes a ground state in which the interaction between the Higgs field and matter (fermion fields) is nonzero, giving rise to the familiar mass terms that we observe in relativistic energy functions. Let us now take a closer look at this vacuum state in which we live.
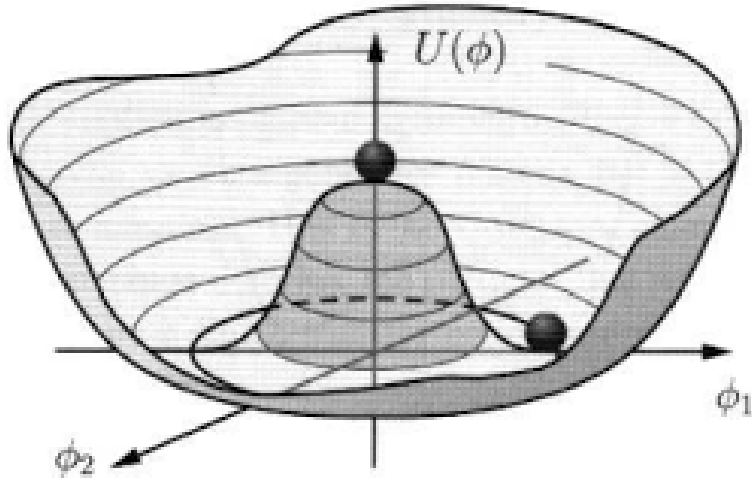
Figure 3.1: The Higgs potential, commonly referred to as the "Mexican hat" potential, $U(\phi) = -\frac{1}{2}\kappa^2\phi^2 + \frac{1}{4}\lambda\phi^4$.

Firstly, it is clear that $\vec{E} = 0$ in the vacuum state, as this minimizes the energy function presented in Eq.(7). In other words, the vacuum expectation value of the electromagnetic field is zero. This takes care of the first, second, and fourth terms in the energy density function. We are then left with

$$u = \frac{d}{d\mathcal{V}}a\Phi - \kappa^2\phi^2 + \lambda\phi^4. \tag{8}$$

But for what Higgs field value is the remainder of this energy function minimized? Let us briefly examine the Higgs potential illustrated in Figure 3.1, describing the omnipresent Higgs field. This function, which only focuses on the Higgs field, only contains Higgs self-interactions, and does not include interactions with fermions. The Higgs potential and its derivative are as follows:

$$
\begin{aligned}
V(\phi) &= -\frac{1}{2}\kappa^2\phi^2 + \frac{1}{4}\lambda\phi^4; \tag{9}\\
V'(\phi) &= -\kappa^2\phi + \lambda\phi^3 \\
&= \phi(-\kappa^2 + \lambda\phi^2). \tag{10}
\end{aligned}
$$

18

Note that we have added constants before each term without loss of generality to simplify the expression of the derivative. Now, setting the derivative to zero in order to obtain the function's minimum, and recognizing that the field's vacuum expectation value is nonzero, we obtain

$$-\kappa^2 + \lambda\phi_0^2 = 0 \tag{11}$$

$$\Rightarrow \langle\phi_0\rangle = \frac{\kappa}{\sqrt{\lambda}}. \tag{12}$$

Thus, the minimum of the Higgs potential illustrated in Figure 3.1 occurs at $\langle\phi_0\rangle = \kappa/\sqrt{\lambda}$.

Let us now return to the energy density function for a particle in a Higgs field and express the Higgs field as the ground state with a perturbative term.

$$u = \frac{d}{d\mathcal{V}}a(\Phi_0 + \Phi') - \kappa^2(\phi_0 + \phi')^2 + \lambda(\phi_0 + \phi')^4 \tag{13}$$

Physically, the ground state ϕ_0 represents the Higgs field which surrounds us, while a perturbation ϕ' of this field represents a physical Higgs particle.

Let us now focus our attention on the first term in Eq.(13). This generalized term represents the interaction between the particle (a fermionic particle, represented by $\frac{d}{d\mathcal{V}}$) with the Higgs field—represented by Φ_0—and with any Higgs particles, represented by Φ'. If we try to explain Einstein's mass term now as an interaction with the Higgs field, we draw the following conclusion:

$$\frac{d}{d\mathcal{V}}mc^2 = \frac{d}{d\mathcal{V}}a\Phi_0 \tag{14}$$

Equivalently,

$$a = \frac{mc^2}{\Phi_0}. \tag{15}$$

Conventionally, the Higgs vacuum expectation value is denoted $v = \sqrt{2}\Phi_0$, and its approximate value is $v = 246$ GeV. Furthermore, we absorb c^2 into the coupling constant a.

Therefore, the coupling constant of an arbitrary fermion to the Higgs field directly relates to its mass, with

$$g = \frac{\sqrt{2}m}{v}.$$
(16)

However, the story does not end there. As we will soon see, higher energies allow for more complex interactions with more virtual particles (which can be thought of as intermediate steps). This complicates matters, as this changes the value of the coupling "constants". For this reason, this relationship is merely approximate. When we are interested in processes which allow for very large energies, the coupling parameters are no longer constant, but rather "run" with the energy scale. We must therefore modify our methods, just as we do when accounting for general relativity when allowing for very large velocities. The formulas describing these coupling parameters at large energy scales are referred to as renormalization group equations, and are discussed in greater detail in section 3.3.

3.2   The Standard Model as a gauge field theory

The Standard Model is a quantum field theory—it defines quantum fields which exist throughout space. Observable particles are manifestations of excited states of these quantum fields.

The quantum fields contained within the Standard Model are:

- electroweak boson fields W_1, W_2, W_3 and B;

- the gluon field G_a,

- the Higgs field ϕ, and

- fermion fields ψ.

Because the Higgs mechanism breaks electroweak symmetry, the electroweak boson states

20

that we observe physically are a "mix" of W_1, W_2, W_3 and B. The observable electroweak bosons are

$$W^\pm = \frac{1}{\sqrt{2}}(W_1 \mp W_2), \tag{17}$$

$$Z = W_3 \cos\theta_W - B \sin\theta_W, \tag{18}$$

$$\gamma = W_3 \sin\theta_W + B \cos\theta_W, \tag{19}$$

where θ_W is the Weinberg angle.

As well as being described as a quantum field theory, the Standard Model is a gauge theory. The model is defined by an internal symmetry that governs the forces of the model. The local gauge symmetry is defined mathematically as

$$G = SU(3)_C \times SU(2)_W \times U(1)_Y. \tag{20}$$

Each of these three symmetry groups acts on fermions, but only selectively on the gauge bosons. For example, only $SU(2)_W$ and $U(1)_Y$ act on ϕ—this is what causes the Higgs mechanism to break electroweak symmetry.

The $SU(3)_C$ "colour" group acts on G, which forms a 3 by 3 rotation matrix whose determinant must be equal to one. This results in 8 gluons. Quarks, on the other hand, are three-component vectors in this $SU(3)$ colour space. The gluons transform these vectors by acting on them; the $SU(3)_C$ gauge is then said to rotate these vectors in colour space. Anti-quarks carry the conjugate colours.

The $SU(2)_W$ "weak isospin" group acts on both W and ϕ, while the $U(1)_Y$ "weak hypercharge" group acts on B and ϕ. The mixing of these gauge fields results in the electroweak theory.

One important feature of the fermion fields is that they are split into two "chirality" components that we call left-handed and right-handed fermions

$$\psi^L = \frac{1}{2}(1 - \gamma_5)\psi, \tag{21}$$

$$\psi^R = \frac{1}{2}(1 + \gamma_5)\psi, \tag{22}$$

where

$$\gamma_5 = \begin{pmatrix} 0 & 0 & 1 & 0 \\ 0 & 0 & 0 & 1 \\ 1 & 0 & 0 & 0 \\ 0 & 1 & 0 & 0 \end{pmatrix} \tag{23}$$

is the fifth gamma matrix.

These left-handed and right-handed fermions transform differently under the gauge symmetries: left-handed fermions transform as doublets under $SU(2)_W$, while right-handed fermions transform as singlets (their weak isospin is always zero). This means that the weak interaction could rotate a left-handed lepton into a muon—with the emission of a W^-—or one flavor of quark into another, but such interactions are impossible with right-handed fermions.

As outlined above, the electroweak gauge that we observe results from the "mixing" of the weak isospin and weak hypercharge gauges. The non-zero Higgs field vacuum expectation value results in the constant interaction of ϕ with the W and B fields, even in vacuum, contributing an inherent "offset" to the weak isospin and weak hypercharge. The relation between the eigenvalue that we observe from this electroweak gauge (electric charge), and the weak isospin and weak hypercharge quantum numbers is

$$Q = T_3 + \frac{Y}{2}, \tag{24}$$

where Q is the electric charge, T_3 is the third component of the weak isospin ($+1/2$ for left-handed up-type quarks and charged leptons, $-1/2$ for left-handed down-type quarks and neutrinos, $+1$ for W^+ and -1 for W^-) and Y is the weak hypercharge.

Having now described all of the fields and interactions of the Standard Model, we can write the Lagrangian in order to mathematically describe the Standard Model in only one formula. The simplified Lagrangian takes on the following form [31]:

$$
\begin{aligned}
\mathcal{L} \quad = \quad & -\frac{1}{4}\sum_{C=1}^{8} G^C_{\mu\nu}G^{C\mu\nu} - \frac{1}{4}\sum_{\alpha=1}^{3} W^\alpha_{\mu\nu}W^{\alpha\mu\nu} - \frac{1}{4}B_{\mu\nu}B^{\mu\nu} \\
& + D^\mu\phi^\dagger D_\mu\phi - V(\phi^\dagger\phi) \\
& + \sum_{n,i,\alpha} iQ^\dagger_{ni\alpha}\bar{\sigma}^\mu D_\mu Q_n^{i\alpha} + \sum_{n,i} iK^{\dagger i}_n\bar{\sigma}^\mu D_\mu K_{ni} \\
& + \sum_{n,\alpha} iL^\dagger_{n\alpha}\bar{\sigma}^\mu D_\mu L_n^\alpha + \sum_{n} iN^\dagger_n\bar{\sigma}^\mu D_\mu N_n \\
& + \mathcal{L}_{Yukawa} + \mathcal{L}_{neutrino\,masses},
\end{aligned}
\tag{25}
$$

where

$$
V(\phi^\dagger\phi) = -\frac{1}{2}\kappa^2\phi^\dagger\phi + \frac{1}{4}\lambda(\phi^\dagger\phi)^2,
\tag{26}
$$

D_μ stands for the covariant derivative, Q_n are the left-handed quark multiplets (their hermitian conjugates $Q^\dagger_n$ form the right-handed antiquarks), K_n are the left-handed antiquark multiplets (their hermitian conjugates $K^\dagger_n$ form the right-handed quarks), L_n and $L^\dagger_n$ are the left-handed leptons and right-handed antileptons respectively, and N_n and $N^\dagger_n$ are the left-handed antileptons and right-handed leptons respectively. The $\mathcal{L}_{Yukawa}$ term refers to the mass terms of the quarks and leptons, while the $\mathcal{L}_{neutrino\,masses}$ term refers to neutrino mass terms, which involve interactions with two Higgs fields, such as allowed by the two-Higgs models explored in this thesis.

3.3 Renormalization Group Equations

The Feynman diagrams introduced in Chapter 2 are complemented by a rather complex mathematical formalism known as the Feynman rules. Given any Feynman diagram, the Feynman rules can then be used to calculate things such as decay rates and scattering amplitudes and cross-sections. In essence, each vertex and propagator in the Feynman diagram adds a factor following an explicit set of rules. Vertices, which represent interactions between particles, provide factors containing coupling constants, while propagators give rise to integrations over the momenta of the traveling particles.

Because we will be looking at coupling constants, which tell us a lot about a particle and how it interacts with other particles, and because these coupling constants are properties of Feynman diagrams, we must in principle consider all the relevant (one-loop) diagrams to the particles of interest. For more precision but at the cost of more lengthy and complex calculations, one can account for more "loops" (particle decays and annihilations contained within a Feynman diagram that do not affect the outcome of the interaction).

It is important to acknowledge that the term "coupling constant" is a bit of a misnomer, as in fact coupling constants have an energy dependence, and therefore they are not fixed for every given pair of particle types. However, when we deal with typical interaction problems, we are only interested in a narrow energy scale. Therefore, for this purpose, coupling constants are fixed. However, because the aim of this thesis deals with the generalization of all interactions within the Standard Model as a whole and effectively with probing the broad range of energies allowed by the Standard Model, we must consider the "running" of coupling parameters with the energy scale.

This running of couplings is described in the form of renormalization group equations (RGEs). The underlying process consists of repeatedly separating finite quantities from divergences caused by infinities resulting from integrating over all possible momenta for the loop and setting these divergences to zero. This process is known as renormalization. The

result is a differential equation describing the running of the coupling constant with the energy scale.

The RGEs associated with the models discussed in this thesis arise from the framework established in a three-part paper written by Marie E. Machacek and Michael T. Vaughn, which details the procedure for formulating RGEs for a general quantum theory [32, 33, 34].

3.4 Problems with the Standard Model

Despite the Standard Model being the most successful theory in particle physics to date, having predicted the existence of the Higgs boson, the $W^{\pm}$ and Z bosons, the gluon, and the top and charm quarks, the Standard Model does have a few major shortcomings. These deficiencies have enticed many particle physicists to study extensions of the Standard Model containing new particles and new physics, and others still to formulate entirely new models such as string theory.

Arguably the most troubling failure of the Standard Model is the complete absence of gravity. The Standard Model has so far been able to describe all of the known forces in terms of particle interactions with the exception of gravity. Not only has the graviton never been proven to exist, but particle physics and general relativity are entirely incompatible, forcing us to treat the microscopic and macroscopic scales completely differently. When faced with microscopic particles, we deal in quantum mechanics and probabilities and uncertainties, whereas with macroscopic celestial bodies, interactions are governed by smooth and well-defined spatial geometry. The ways in which systems behave at these two vastly different scales seem entirely independent of one another. The most successful quantum gravity theory candidates typically consist of different veins of string theory [35], however these theories are purely theoretical and prove difficult, if not impossible, to confirm experimentally.

Another major shortcoming of the Standard Model is its inability to explain the nature of dark matter and dark energy. According to the laws of gravity, the solar systems closest

to the centre of our galaxy should orbit the centre at a higher speed than those on the outer edges, however in reality, they all travel at roughly the same speed. This is what lead cosmologists to formulate the existence of a halo of "dark matter" surrounding our galaxy—some unknown source of gravitation exerting an extra pull on solar systems within the outer reaches of the galaxy. While dark matter attracts celestial bodies within galaxies, dark energy repels on a much larger cosmic scale. It is responsible for the expansion of the universe, which, like dark matter, has remained yet unexplained. Of all the particles contained in the Standard Model, none have the properties of dark matter nor dark energy. To reconcile this, many physicists simply theorize the existence of undiscovered particles bearing the properties of dark matter [22, 36], while others have formulated a theory in which dark matter is actually a consequence of a hidden multiverse interacting with our own universe, and that gravity can in fact "leak" between universes [37].

Another percepted problem arises from symmetry. The Standard Model presents several seemingly arbitrary asymmetries that remain unexplained. While not all physicists take issue with this, many others have an intuition-based desire to observe symmetries in nature and insist that such asymmetries must have logical explanations waiting to be discovered. One such asymmetry that remains a mystery is the matter-antimatter asymmetry; it is widely assumed that the Big Bang should have produced matter and antimatter in equal amounts, however there is an obvious imbalance in favour of matter. Analyses have been performed which consider whether or not matter and antimatter could be simply separated into different regions of the universe [38], however it is deemed unlikely that such regions dominated by antimatter exist. The general consensus on this matter is that charge, parity, and time-reversal symmetry violations in certain weak interactions are responsible for creating different decay rates for opposing reactions, resulting in the production of more matter than antimatter after the Big Bang [39, 40, 41].

Finally, vacuum instability, the flaw that serves as a primary motivation and focus of this thesis, stems from the recent discovery of the Higgs boson, or more specifically, with its mass, as we will show in the following chapter. The result of this flaw, however, is that

the Standard Model fails at energies above 10^6GeV, requiring new physics at this scale. In order to be satisfied that we have a complete theory of physics, we require coverage up to Planck scale, which is considered the universal physical limit.

Chapter 4

Vacuum stability in the Standard Model

Gaining much public attention after its discovery at CERN in 2012, the Higgs boson's role is to act as a mediator of the Higgs field, which is responsible for assigning mass to all of the elementary particles described by the Standard Model. These particle masses are directly proportional to the strength of their interactions with the Higgs boson:

$$m_i = \frac{y_i v}{\sqrt{2}}, \tag{27}$$

where $v = 246\text{GeV}$ is the Higgs vacuum expectation value and y_i is the coupling constant of the interaction of the Higgs with the elementary particle in question.

Interactions with the Higgs field are specified by the Higgs potential, which has the form

$$V(\phi) = -\frac{1}{2}\kappa^2\phi^2 + \frac{1}{4}\lambda\phi^4 + \mathcal{O}(\phi^6), \tag{28}$$

where κ and λ are renormalized quantities and ϕ is the value of the Higgs field. Vacuum stability requires the Higgs field in vacuum to be located at a global minimum in the
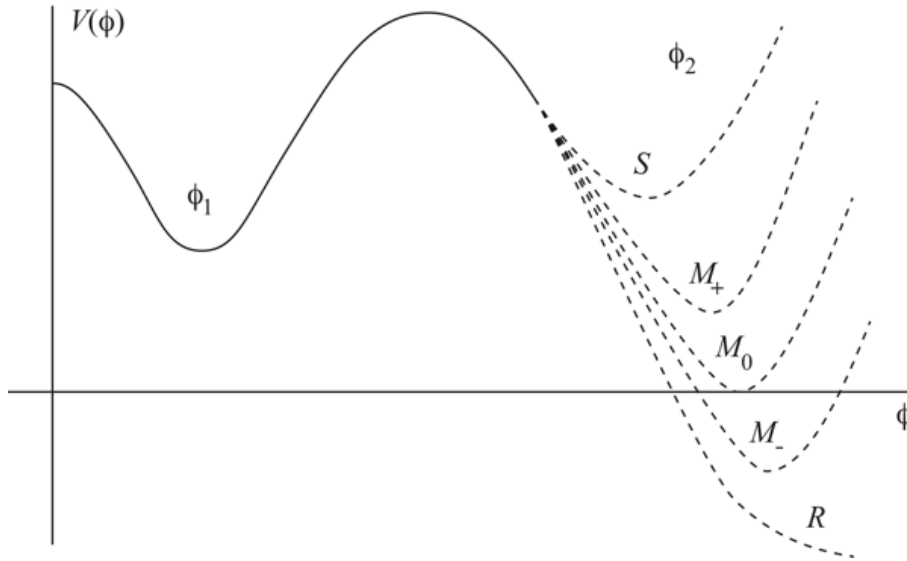
Figure 4.1: The Higgs potential as a function of the value of the Higgs field.

potential, or, alternatively, $\lambda(\mu) > 0$, where λ is the "running" quadratic Higgs self-coupling parameter, which varies with the energy scale μ at which the Standard Model breaks down.

Figure 4.1 illustrates the energy of the Higgs field as a function of the field value ϕ. If the ground state of our universe (labeled ϕ_1) exists in a global minimum (all other minimums, if they exist, are at higher energies, as illustrated by local minimum S), then the vacuum is said to be stable, and the physical implication is that the universe will keep inflating eternally. However, if, on the other hand, there exists a lower minimum as illustrated by local minima M_+, M_0 and M_- in Figure 4.1, then there is a very small chance at any given moment that our vacuum expectation value could quantum tunnel through the potential to the other vacuum expectation value ϕ_2. The probability of this occurring depends on the height and width of the "hill" in the potential energy function between the two minima, and given the age of our universe, this probability would be very low, meaning that our universe would continue to exist as it is for trillions of years, however eventually, over a long enough time, the nonzero probability of this collapse would ensure the inevitable total destruction and rebirth of our universe, beginning at a particular point in space and propagating at the speed of light. This scenario in which there exists a lower energy minimum is referred to as meta-stability, as the universe is long-lived, however not infinitely. It is furthermore

interesting to note that should the energy in the other state be negative, as indicated by M_-, the fabric of our spacetime will collapse into a Big Crunch, as opposed to inflating as with M_+. In the zero-energy case of M_0, the universe will neither expand nor collapse, and this also has other major implications with regards to the Standard Model as the Higgs mechanism is not possible with a zero Higgs vacuum expectation value.

We now return our focus to the SM Higgs potential. Whether stable or meta-stable, we require $\lambda > 0$ locally in order to give us the local minimum in which the vacuum state of our universe exists. The only question is, at what scale does the Standard Model break down? In order for the Standard Model to be a complete physical theory, we require it to be valid up to Planck scale, or 10^{18} GeV, as this is the universal limit of physical relevance. If the Standard Model is not valid up to Planck scale, then we require new physics and the SM can only serve as an approximation, and not a completely accurate theory. However, the simpler solution that we will offer here is the existence of new particles rather than new physics. With this simple solution comes the assumption that the Standard Model is effective up to Planck scale, i.e. $\lambda > 0$ for $\mu \leq 10^{18}$ GeV.

We will now study what this vacuum stability means for the Higgs mass. In order to study the self-coupling parameter λ across all energy scales, we must make use of the RGE given in [42] as follows:

$$\frac{d\lambda(\mu)}{d\ln\mu} = \frac{1}{16\pi^2}\left[4\lambda^2 + 12\lambda y_t^2 - 36y_t^4 - 9\lambda g_1^2 - 3\lambda g_2^2 + \frac{9}{4}g_2^4 + \frac{9}{2}g_1^2 g_2^2 + \frac{27}{4}g_1^4\right] \qquad (29)$$

Here and in the future, $g_i = \{g_1, g_2, g_3\}$ are coupling parameters of the Higgs to the U(1), SU(2), and SU(3) gauges respectively, each of these symmetry groups representing the three fundamental forces described by the SM. y_t, on the other hand, represents the coupling of the Higgs to the top quark. We refer to couplings involving the Higgs boson collectively as Yukawa couplings. All coupling parameters depend on the possible intermediate interactions, which in turn depend on the upper energy limit. For this reason, coupling parameters are renormalized and can be thought of as "running" as a function of the energy scale μ and

as such, we must consider their renormalization group equations, such as the one presented in Eq.(29).

The renormalization group equations for the gauge bosons and top quark in the SM are well-known and can be found in [43]. For the top quark Yukawa coupling, we have

$$\frac{dy_t(\mu)}{d\ln\mu} = \frac{y_t}{16\pi^2}\left[\frac{9}{2}y_t^2 - \frac{9}{4}g_2^2 - \frac{17}{12}g_1^2 - 8g_3^2\right],\tag{30}$$

and for the gauge couplings $g_i = \{g_1, g_2, g_3\}$, we have

$$\frac{dg_i(\mu)}{d\ln\mu} = \frac{1}{16\pi^2}b_i g_i^3, \; b = (41/6, -19/6, -7).\tag{31}$$

At small energy scales, the gauge couplings may be thought of as coupling constants, and the top Yukawa coupling in particular can be expressed in terms of the top mass. Since these coupling parameters run at increasing energies, these constant values serve as initial conditions to the renormalization group equations. They are written explicitly as

$$g_1^2(\mu_0) = 4\pi\alpha,\tag{32}$$

$$g_2^2(\mu_0) = 4\pi\alpha\left(\frac{1}{\sin\theta_W} + 1\right),\tag{33}$$

$$g_3^2(\mu_0) = 4\pi\alpha_s,\tag{34}$$

$$y_t(\mu_0) = \frac{\sqrt{2}m_t}{v},\tag{35}$$

$$\lambda(\mu_0) = \frac{3m_H^2}{v^2}[1 + \delta_\lambda(\mu_0)],\tag{36}$$

The relevant constants in the above equations are all well-known: the fine-structure constant is $\alpha = e^2/4\pi\epsilon_0\hbar c = 1/137$, the strong coupling is $\alpha_s = 0.118$, the Weinberg angle or weak mixing angle is $\sin\theta_W = 0.2312$, the Higgs vacuum expectation value is $v = 246.22$ GeV, and the top quark and Higgs boson masses are 174 GeV and 125 GeV, respectively. We set the beginning of the running of the couplings at $\mu_0 = m_Z = 91.188$ GeV.

By solving this set of differential equations and initial conditions, we may obtain $\lambda(\mu)$ at

31

any given energy scale. The radiative correction term δ_λ is defined in [44] as

$$\delta_\lambda(\mu) = \frac{G_F}{\sqrt{2}} \frac{m_Z^2}{8\pi^2} \left[\xi f_1(\xi, \mu) + f_0(\xi, \mu) + \xi^{-1} f_{-1}(\xi, \mu) \right], \tag{37}$$

where $G_F = 1.16635 \times 10^{-5} \text{GeV}^{-2}$ is the muon decay coupling constant, $\xi \equiv m_H^2/m_Z^2$, and

$$
\begin{aligned}
f_1(\xi, \mu) &= 6\ln\frac{\mu^2}{m_H^2} + \frac{3}{2}\ln\xi - \frac{1}{2}Z\left(\frac{1}{\xi}\right) - Z\left(\frac{c^2}{\xi}\right) - \ln c^2 + \frac{9}{2}\left(\frac{25}{9} - \sqrt{\frac{1}{3}}\pi\right), \tag{38}\\
f_0(\xi, \mu) &= -6\ln\frac{\mu^2}{m_Z^2}\left[1 + 2c^2 - 2\frac{m_t^2}{m_Z^2}\right] + \frac{3c^2\xi}{\xi - c^2}\ln\frac{\xi}{c^2} + 2Z\left(\frac{1}{\xi}\right)\\
&\quad + 4c^2 Z\left(\frac{c^2}{\xi}\right) + \frac{3c^2\ln c^2}{s^2} + 12c^2\ln c^2 - \frac{15}{2}(1 + 2c^2)\\
&\quad - 3\frac{m_t^2}{m_Z^2}\left[2Z\left(\frac{m_t^2}{m_Z^2\xi}\right) + 4\ln\frac{m_t^2}{m_Z^2} - 5\right], \tag{39}\\
f_{-1}(\xi, \mu) &= 6\ln\frac{\mu^2}{m_Z^2}\left[1 + 2c^4 - 4\frac{m_t^4}{m_Z^4}\right] - 6Z\left(\frac{1}{\xi}\right) - 12c^4 Z\left(\frac{c^2}{\xi}\right) - 12c^4\ln c^2\\
&\quad + 8(1 + 2c^4) + 24\frac{m_t^4}{m_Z^4}\left[\ln\frac{m_t^2}{m_z^2} - 2 + Z\left(\frac{m_t^2}{m_Z^2\xi}\right)\right], \tag{40}
\end{aligned}
$$

$$
\begin{aligned}
Z(z) &= \begin{cases} 2A\tan^{-1}(1/A), & (z > 1/4)\\ A\ln\left[(1 + A)/(1 - A)\right], & (z < 1/4), \end{cases}\\
A &\equiv |1 - 4z|^{1/2}, \tag{41}
\end{aligned}
$$

where c^2, s^2 are abbreviations for $\cos^2\theta_W$ and $\sin^2\theta_W$. The functions f_{-1}, f_0, and f_1 are defined in [44].

The dependence of the Higgs coupling λ as a function of the energy scale μ is plotted in Figure 4.2 for different values of m_H. Furthermore, if we fix $\lambda = 0$ and instead leave m_H unspecified, we examine the lower limit on the Higgs mass as a function of μ, illustrated for different values of m_t in Figure 4.3. It is apparent that the exact mass of the top quark greatly affects the bound on the Higgs mass. Since the top quark is the heaviest quark known to the SM, we expect its interaction with the Higgs to be proportionally large from
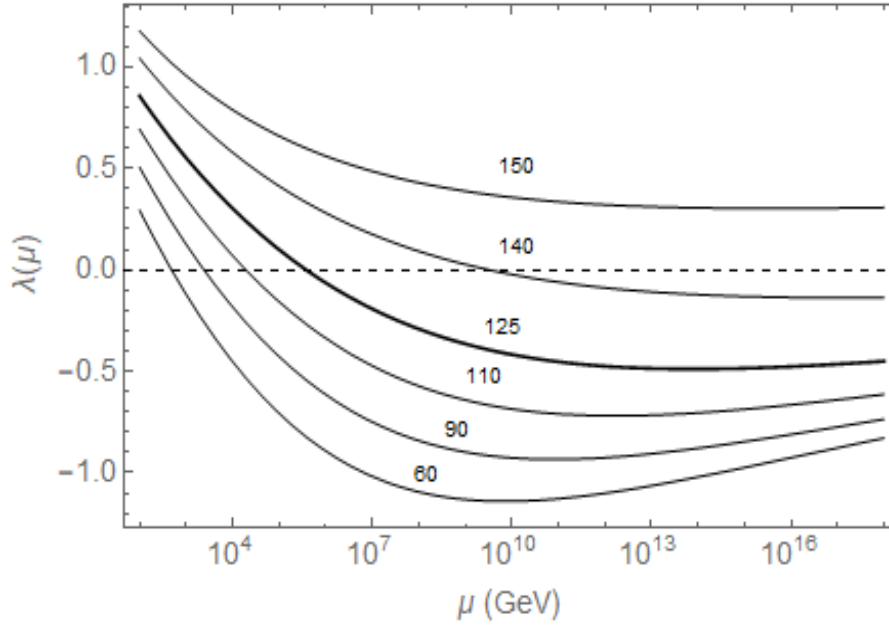
Figure 4.2: The Higgs coupling as a function of μ for different values of m_H. The Higgs mass of 125 GeV as measured experimentally by CERN is given in bold.

Eq.(27).

Both Figures 4.2 and 4.3 compare quite well with the results illustrated in [42], however the Higgs bound for $m_t = 210$ GeV could not be computed explicitly for larger values of μ due to a singularity in λ near $m_H = 155$ GeV and instead, extrapolation was used, explaining the discrepancy in Figure 4.3.

It is clear from Figure 4.2 that the Higgs potential de-stabilizes around 10^6 GeV, and that this instability disappears at larger Higgs mass values. It is for this reason that the expected mass of the Higgs before its experimental discovery was significantly higher than the observed value. This stability problem requires additional particles in the SM, or new physics before Planck scale (just as, for example, Einstein's theory of special relativity came to the rescue of Newtonian physics).

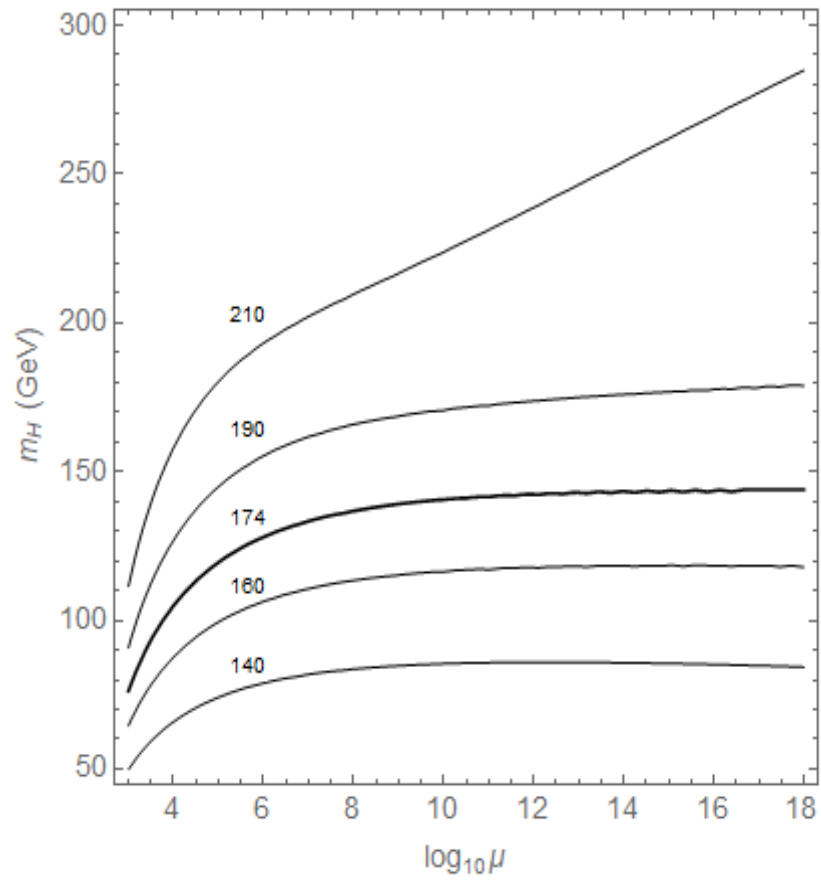Figure 4.3: Lower limits on m_H as a function of μ for different values of m_t. The experiementally determined mass of the top quark of 174 GeV is given in bold.

Chapter 5

Vacuum stability in minimal two-Higgs extensions

5.1 Vacuum stability in a two-Higgs model

In this section, we consider an extension of the SM containing an extra scalar boson singlet (a new Higgs-like particle) which interacts solely with the SM Higgs, and we examine the constraints placed on the mass and mixing angle of this hypothetical particle by the Higgs vacuum stability condition. It is worth mentioning that the addition of fermions to the SM has a negative contribution to the Higgs quartic coupling as we will show in the next chapter, thus exacerbating the Higgs vacuum instability problem. The addition of bosons, on the other hand, provides a positive boost to the coupling parameter, and so all of the SM extensions that we will study in this thesis will contain an extra scalar boson, with the goal of repairing the Higgs vacuum stability. We begin with the simplest case, namely the sole addition of this extra boson, and in the following sections we consider extensions containing this extra boson as well as different fermion generations.

In this model, the Higgs doublet Φ and the new singlet scalar boson χ interact with one

another in addition to themselves, and thus the Higgs sector potential, to the fourth order, has the following form:

$$V(\Phi, \chi) = -\mu_H^2 \Phi^\dagger \Phi + \lambda_H (\Phi^\dagger \Phi)^2 - \frac{\mu_S^2}{2} \chi^2 + \frac{\lambda_S}{4} \chi^4 + \frac{\lambda_{SH}}{2} (\Phi^\dagger \Phi) \chi^2. \tag{42}$$

Just as in the SM case, we require $\lambda_H > 0$ in order to obtain the "Mexican hat" potential allowing for a stable vacuum. In addition, we require $\lambda_S > 0$ so that the potential associated with the new particle may have the same form. In fact, requiring the potential to be positive for asymptotically large values of the fields, we obtain the following conditions:

$$\lambda_H > 0, \qquad 0 < \lambda_S < 4\pi, \qquad |\lambda_{SH}| < 4\pi. \tag{43}$$

As we have seen earlier, the mass of a particle is intimately related to these coupling parameters. As a result of the electroweak symmetry breaking, there is mass mixing between the SM Higgs ϕ and the new scalar χ. The mixing matrix, given in [23], is

$$\mathcal{M}_S^2 = \begin{pmatrix} 2\lambda_H v^2 & \lambda_{SH} vu \\ \lambda_{SH} vu & 2\lambda_S u^2 \end{pmatrix}, \tag{44}$$

where v is the vacuum expectation value of the SM Higgs field, and u is that of the new Higgs-like scalar field. The mass eigenvalues can then be obtained by diagonalizing the mixing matrix. This yields

$$m_{H,S}^2 = \lambda_H v^2 + \lambda_S u^2 \mp \sqrt{(\lambda_S u^2 - \lambda_H v^2)^2 + \lambda_{SH}^2 u^2 v^2}, \tag{45}$$

and the eigenvectors are

$$\begin{pmatrix} H \\ S \end{pmatrix} = \begin{pmatrix} \cos\phi & -\sin\phi \\ \sin\phi & \cos\phi \end{pmatrix} \begin{pmatrix} \Phi \\ \chi \end{pmatrix}, \tag{46}$$

36

where the mass mixing angle is given by

$$\tan 2\phi = \frac{\lambda_{SH} uv}{\lambda_S u^2 - \lambda_H v^2}. \tag{47}$$

From Eqs. (45) & (47), we can express the coupling parameters in terms of the masses,

$$\lambda_H = \frac{m_H^2 \cos^2 \phi + m_S^2 \sin^2 \phi}{2v^2}, \tag{48}$$

$$\lambda_S = \frac{m_S^2 \cos^2 \phi + m_H^2 \sin^2 \phi}{2u^2}, \tag{49}$$

$$\lambda_{SH} = \frac{m_S^2 - m_H^2}{2uv} \sin 2\phi. \tag{50}$$

Of course, we wish for these conditions to hold true for all scales up to Planck scale (10^{18} GeV). So, in order to know these coupling parameters at higher energy scales, we require the RGEs for the model, which are given in [23]. Just like Xiao and Yu, we have taken the starting point of the running to be $\mu_0 = m_t$.

The Yukawa and Higgs sector RGEs are

$$\frac{dy_t^2}{d\ln\mu^2} = \frac{y_t^2}{(4\pi)^2} \left(\frac{9y_t^2}{2} - \frac{17g_1^2}{20} - \frac{9g_2^2}{4} - 8g_3^2 \right), \tag{51}$$

$$\frac{d\lambda_H}{d\ln\mu^2} = \frac{1}{(4\pi)^2} \left[\lambda_H \left(12\lambda_H + 6y_t^2 - \frac{9g_1^2}{10} - \frac{9g_2^2}{2} \right) \right.$$
$$\left. + \left(\frac{\lambda_{SH}^2}{4} - 3y_t^4 + \frac{27g_1^4}{400} + \frac{9g_2^4}{16} + \frac{9g_1^2 g_2^2}{40} \right) \right], \tag{52}$$

$$\frac{d\lambda_S}{d\ln\mu^2} = \frac{1}{(4\pi)^2} \left(9\lambda_S^2 + \lambda_{SH}^2 \right), \tag{53}$$

$$\frac{d\lambda_{SH}}{d\ln\mu^2} = \frac{\lambda_{SH}}{(4\pi)^2} \left(2\lambda_{SH} + 6\lambda_H + 3\lambda_S + 3y_t^2 - \frac{9g_1^2}{20} - \frac{9g_2^2}{4} \right), \tag{54}$$

where λ_H and λ_S are the Higgs and new scalar quartic self-couplings, respectively, and λ_{SH} is the coupling of the two together. Eqs. (48)–(50) describe the coupling parameters at relatively small energy scales, and therefore serve as initial conditions to these RGEs. Note that just as with the SM, we ignore the contributions of all Yukawa couplings except for

37

that of the top quark, due to their negligible masses and thus negligible contributions to the Higgs sector couplings.

Just as in the SM, and as we will continue to do for each of the models studied in this thesis, we include electroweak radiative correction terms for increased accuracy. To this end, we replace the top Yukawa coupling and Higgs self-coupling boundary conditions with

$$y_t = \frac{\sqrt{2}m_t}{v}[1 + \Delta_t(\mu_0)], \tag{55}$$

$$\lambda_H = \frac{m_H^2 \cos^2 \phi + m_S^2 \sin^2 \phi}{2v^2}[1 + \Delta_H(\mu_0)], \tag{56}$$

where $\Delta_H(\mu)$ is the same correction term used in the SM case obtained from [44], and $\Delta_t(\mu)$ is given in [45] as a sum of terms corresponding to a contribution of each of the bosonic interactions (weak, electromagnetic, and strong), i.e.

$$\Delta_t(\mu_0) = \Delta_W(\mu_0) + \Delta_{QED}(\mu_0) + \Delta_{QCD}(\mu_0), \tag{57}$$

$$\Delta_{QED}(\mu_0) = \frac{\alpha}{9\pi}\left(3\ln\frac{m_t^2}{\mu_0^2} - 4\right), \tag{58}$$

$$\Delta_{QCD}(\mu_0) = \frac{\alpha_s}{3\pi}\left(3\ln\frac{m_t^2}{\mu_0^2} - 4\right), \tag{59}$$

$$\Delta_W(\mu_0) = \frac{G_F m_t^2}{16\pi^2\sqrt{2}}\left(-9\ln\frac{m_t^2}{\mu_0^2} - 4\pi\frac{m_H}{m_t} + 11\right), \tag{60}$$

where we recall that $\alpha = 1/137$ is the fine-structure constant, $\alpha_s = 0.118$ is the strong-coupling constant, and $G_F = 1.16635 \times 10^{-5} \text{GeV}^{-2}$ is the Fermi coupling constant. These initial conditions are again evaluated at $\mu_0 = m_t$.

The gauge couplings, responsible for the force-carrying boson interactions, run with the

energy scale according to the gauge coupling RGEs

$$\frac{dg_1^2}{d\ln\mu^2} = \frac{g_1^4}{(4\pi)^2}\left(\frac{41}{10}\right),$$ (61)

$$\frac{dg_2^2}{d\ln\mu^2} = \frac{g_2^4}{(4\pi)^2}\left(-\frac{19}{6}\right),$$ (62)

$$\frac{dg_3^2}{d\ln\mu^2} = \frac{g_3^4}{(4\pi)^2}(-7).$$ (63)

These gauge coupling RGEs are identical to those that describe the SM; they are unaffected by the addition of the new boson since we assume no coupling between the scalar boson and the SM gauge bosons.
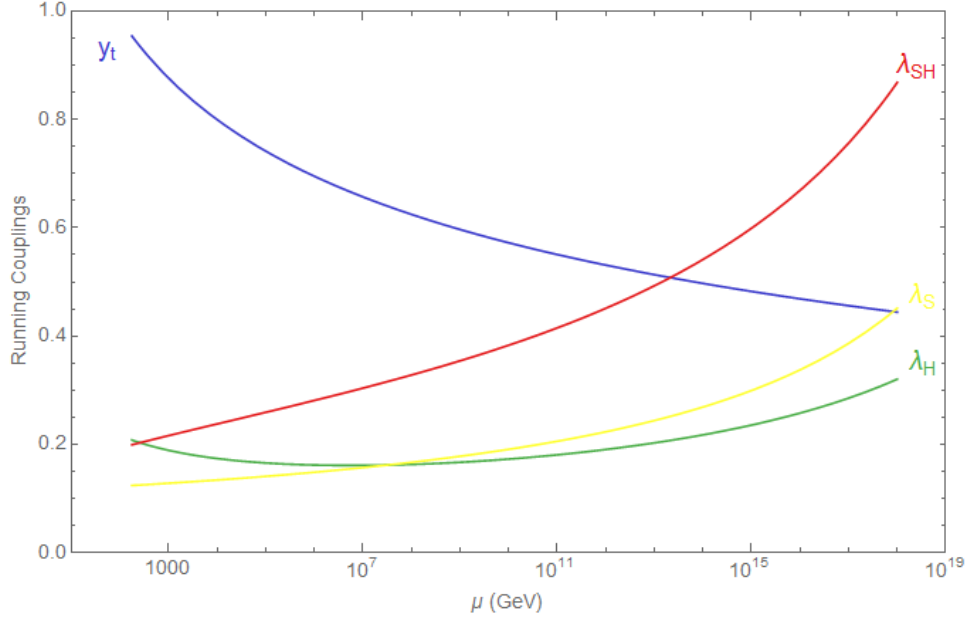
Figure 5.1: The RGE running of the top Yukawa coupling and scalar couplings for the scalar boson model with $m_S = 1$ TeV, $\sin\phi = 0.1$, $u = 2$ TeV, and the starting point of the running is at $\mu_0 = m_t$.

Figure 5.1 illustrates the running of the coupling parameters for a typical set of parameter values. Notice that in this model and for this particular selection of parameter values, the scalar couplings increase with increasing energy scales. Recall that in the SM, the Higgs coupling decreased, becoming negative at $\sim 10^{10}$ GeV. If the SM is indeed meant to describe processes at energies up to Planck scale, then the Higgs coupling must remain positive at all energy scales within this range. Therefore, the addition of an extra scalar boson to the

SM rescues the theory from vacuum instability.

Of course, we may only speculate the mass and mixing angle of this hypothetical particle. We can guess that its mass might be larger than that of the Higgs, as particles with smaller masses are more easily observed experimentally, however we have no other intuitive direction that might illuminate an experimental search for such a particle. We may, however, eliminate all parameter values that do not satisfy Higgs vacuum stability. To do so, we perform a scan over a broad parameter space and check which parameter values satisfy the vacuum stability conditions outlined in Eq.(43). The resulting allowed parameter space is illustrated in Figure 5.2.

(a) $u = 1$ TeV.   (b) $u = 2$ TeV.   (c) $u = 4$ TeV.
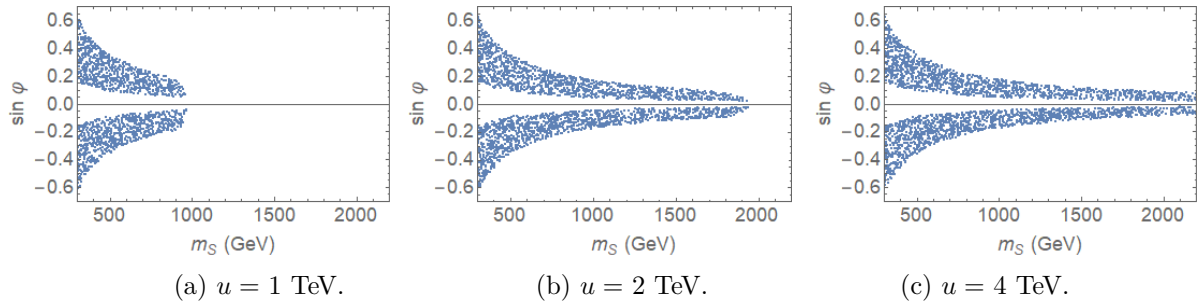
Figure 5.2: The allowed parameter space for the additional scalar boson model for different vacuum expectation values.

We remark that there is necessarily mass mixing between the SM Higgs boson and the new scalar boson, as the region surrounding the axis corresponding to zero mass mixing lies outside of the permitted region. Furthermore, the allowed range for the mass is quite large, particularly if we allow a larger vacuum expectation value. A large mass, of course, would explain why such a particle has not yet been found, as producing heavier particles requires higher energies. Even the Higgs at only 125 GeV, for example, had not been observed until recently in 2012. Fortunately, we may anticipate higher energy collisions at the Large Hadron Collider in the years to come.

5.2 Vacuum stability in a vectorlike fermion two-Higgs model

We now consider an extension of the SM containing a new scalar boson as well as a new vectorlike fermion; this model is the primary focus in [23].

The Yukawa couplings involving this vectorlike fermion ψ and the top quark τ provide the Lagrangian with the following terms:

$$-\mathcal{L}_{Yukawa} = \frac{y_M}{\sqrt{2}}\chi\bar{\psi}_L\psi_R + \frac{\lambda_T}{\sqrt{2}}\chi\bar{\psi}_L\tau_R + y_t\bar{Q}_L\tilde{H}\tau_R + y_T\bar{Q}_L\tilde{H}\psi_R + \text{h.c.} \qquad (64)$$

Here, $\tilde{H} = i\sigma_2 H^*$ represents the Higgs field and Q_L is the left-handed third-generation quark doublet $Q_L = \begin{pmatrix} \tau_L \\ b_L \end{pmatrix}$. Recall that the right-handed SM quarks transform as singlets. Vectorlike fermions, on the other hand, transform in the same way regardless of chirality. For this reason, they obtain a Dirac mass term which, unlike with SM fermions, is not forbidden by any symmetry:

$$-\mathcal{L}_{mass} = m_D\bar{\psi}_L\psi_R + \text{h.c.} \qquad (65)$$

Unlike SM fermions which act as doublets under $SU(2)_W$ if left-handed and as singlets if right-handed, vectorlike fermions have the same interactions regardless of chirality. They appear in many new physics models, such as models with extra dimensions. Unlike SM fermions, these are not ruled out by measurements of the Higgs mass and production cross-section.

Vectorlike fermions, which decay into SM fermions and a gauge boson or a Higgs particle, are predicted by extra-dimensional models [46], little Higgs models [47], string theories and D-brane theories [48] and by some composite Higgs models [49] and they may provide a better fit to the LHC Higgs data [50]. A great deal of literature is dedicated to analyses of vectorlike fermions in the SM [51, 52, 53], as well as in model-independent scenarios [54].

Vectorlike fermions do not acquire mass through Yukawa couplings: In fact, Yukawa interactions involve the presence of both left-handed and right-handed SM fermions. This can be interpreted as a chiral fermion "bumping into" the Higgs field and producing a fermion with the opposite chirality, and so on, so that any given observable fermion represents a mass mixing of two different chiral states. At any given moment, an SM fermion can be measured to be either left-handed or right-handed. It is due to the nature of these Higgs interactions that vectorlike fermions do not acquire mass through the Higgs mechanism like the SM fermions. Instead, non-chiral pairs of fermions are able to achieve mass explicitly through interactions involving only their mirror counterparts [52]. For this reason, their mass scale remains thus far largely unknown.

It is important to note that when we consider the addition of a vectorlike fermion to the Standard Model, the addition of a new scalar boson is necessary to ensure the stability of the Higgs potential. If we try to add the new vectorlike fermion without a new scalar boson, this results in the singular divergence of the Higgs quartic coupling. This is the motivation behind this model as presented by Xiao and Yu. Just as in the previous model, we require the Higgs sector potential given in Eq.(42) to be positive at asymptotically large values of the fields, up to Planck scale.

The gauge coupling renormalization group equations, which describe the interactions between the force-carrying bosons and fermions, gain additional terms in this model due to the new fermion as follows:

$$
\frac{dg_1^2}{d\ln\mu^2} = \frac{g_1^4}{(4\pi)^2}\left(\frac{41}{10}+\frac{16}{15}\right),
\tag{66}
$$

$$
\frac{dg_2^2}{d\ln\mu^2} = \frac{g_2^4}{(4\pi)^2}\left(-\frac{19}{6}\right),
\tag{67}
$$

$$
\frac{dg_3^2}{d\ln\mu^2} = \frac{g_3^4}{(4\pi)^2}\left(-7+\frac{2}{3}\right).
\tag{68}
$$

Here, the second terms in Eqs. (66) and (68) are new terms that come from the added fermion. The SM gauge coupling RGEs are identical to these RGEs minus these two terms.

In this model, we must consider three Yukawa coupling RGEs—where we define Yukawa couplings as the interaction between fermions and either of the two scalar bosons. Here, y_t is the coupling of the top quark to the Higgs field. We call the Higgs coupling of the new vectorlike fermion y_T, and that of the new fermion with the new scalar y_M. We assume that the new scalar does not interact with the top quark for the sake of the model's simplicity, but the top and new fermion mix. Again, we omit the Yukawa couplings of the lighter fermions due to their negligible masses. The relevent Yukawa coupling RGEs are then

$$
\frac{dy_t^2}{d\ln\mu^2} = \frac{y_t^2}{(4\pi)^2}\left(\frac{9y_t^2}{2} + \frac{9y_T^2}{2} - \frac{17g_1^2}{20} - \frac{9g_2^2}{4} - 8g_3^2\right), \tag{69}
$$

$$
\frac{dy_T^2}{d\ln\mu^2} = \frac{y_T^2}{(4\pi)^2}\left(\frac{9y_t^2}{2} + \frac{9y_T^2}{2} + \frac{y_M^2}{4} - \frac{17g_1^2}{20} - \frac{9g_2^2}{4} - 8g_3^2\right), \tag{70}
$$

$$
\frac{dy_M^2}{d\ln\mu^2} = \frac{y_M^2}{(4\pi)^2}\left(y_T^2 + \frac{9y_M^2}{2} - \frac{8g_1^2}{5} - 8g_3^2\right). \tag{71}
$$

And finally, the Higgs sector RGEs (describing interactions involving only the two scalar bosons) are

$$
\begin{aligned}
\frac{d\lambda_H}{d\ln\mu^2} &= \frac{1}{(4\pi)^2}\left[\lambda_H\left(12\lambda_H + 6y_t^2 + 6y_T^2 - \frac{9g_1^2}{10} - \frac{9g_2^2}{2}\right)\right.\\
&\quad \left. + \frac{\lambda_{SH}^2}{4} - 3y_t^4 - 3y_T^4 - 6y_t^2y_T^2 + \frac{27g_1^4}{100} + \frac{9g_2^4}{16} + \frac{9g_1^2g_2^2}{40}\right],
\end{aligned} \tag{72}
$$

$$
\frac{d\lambda_S}{d\ln\mu^2} = \frac{1}{(4\pi)^2}\left(9\lambda_S^2 + \lambda_{SH}^2 + 6y_M^2\lambda_S - 3y_M^4\right), \tag{73}
$$

$$
\begin{aligned}
\frac{d\lambda_{SH}}{d\ln\mu^2} &= \frac{1}{(4\pi)^2}\left[\lambda_{SH}\left(6\lambda_H + 3\lambda_S + 2\lambda_{SH} + 3y_t^2 + 3y_T^2 + 3y_M^2 - \frac{9g_1^2}{20} - \frac{9g_2^2}{4}\right)\right.\\
&\quad \left. - 6y_T^2y_M^2\right].
\end{aligned} \tag{74}
$$

The initial conditions of the Higgs sector couplings are obtained by diagonalization of the mixing matrix in exactly the same way as in the previous model as seen in Eqs.(48)–(50). Along the same vein, we may obtain expressions for the various Yukawa couplings in terms of the mass mixing between the top quark t and the new fermion T, which we call θ_L. The

mass mixing matrix for the vectorlike fermion T and top quark t, as given in [23], is

$$\mathcal{M}_F = \begin{pmatrix} \frac{y_t v}{\sqrt{2}} & \frac{y_T v}{\sqrt{2}} \\ 0 & \frac{y_M u}{\sqrt{2}} \end{pmatrix}. \tag{75}$$

It yields eigenvalues

$$M_{t,T}^2 = \frac{1}{4} \left(y_t^2 v^2 + y_T^2 v^2 + y_M^2 u^2 \right) \left[1 \mp \sqrt{1 - \left(\frac{2 y_t y_M v u}{y_t^2 v^2 + y_T^2 v^2 + y_M^2 u^2} \right)^2} \right] \tag{76}$$

and eigenvectors

$$\begin{pmatrix} t_{L,R} \\ T_{L,R} \end{pmatrix} = \begin{pmatrix} \cos\theta_{L,R} & -\sin\theta_{L,R} \\ \sin\theta_{L,R} & \cos\theta_{L,R} \end{pmatrix} \begin{pmatrix} \tau_{L,R} \\ \Upsilon_{L,R} \end{pmatrix}, \tag{77}$$

where the mixing angles

$$\tan 2\theta_L = \frac{2 y_T y_M v u}{y_M^2 u^2 - y_T^2 v^2 - y_t^2 v^2}, \tag{78}$$

$$\tan 2\theta_R = \frac{2 y_t y_T v^2}{y_M^2 u^2 + y_T^2 v^2 - y_t^2 v^2} \tag{79}$$

are related by

$$\tan\theta_R = \frac{m_t}{m_T} \tan\theta_L. \tag{80}$$

The expressions for the coupling parameters resulting from Eqs. (76) & (78) are

$$y_t(\mu_0) = \frac{\sqrt{2} m_t}{v} \frac{1}{\sqrt{\cos^2\theta_L + x_t^2 \sin^2\theta_L}}, \tag{81}$$

$$y_T(\mu_0) = \frac{\sqrt{2} m_T}{v} \frac{\sin\theta_L \cos\theta_L (1 - x_t^2)}{\sqrt{\cos^2\theta_L + x_t^2 \sin^2\theta_L}}, \tag{82}$$

$$y_M(\mu_0) = \frac{\sqrt{2} m_T}{u} \sqrt{\cos^2\theta_L + x_t^2 \sin^2\theta_L}, \tag{83}$$

where $x_t = m_t/m_T$. We use these expressions to describe the coupling parameters at smaller scales than those at which the parameters are running. As such, these serve as initial conditions to the differential equations listed above.

44

Now that we have all of the RGEs and boundary conditions, we may illustrate the RGE running of the Yukawa and scalar couplings for a typical set of parameter values. Figures 5.3, 5.4, and 5.5 illustrate these couplings for different vacuum expectation values of the new scalar boson field (1 TeV, 2 TeV, and 4 TeV, respectively). In the case of $u = 1$ TeV, we have taken the mass of the scalar boson to be 0.8 TeV, because at 1 TeV, the Higgs sector couplings diverge, leading to singularities. However, on the other hand, in the case of $u = 2$ TeV and $u = 4$ TeV, we take $m_S = 1$ TeV because a smaller mass of 0.8 TeV is not large enough to ensure a positive Higgs quartic coupling.
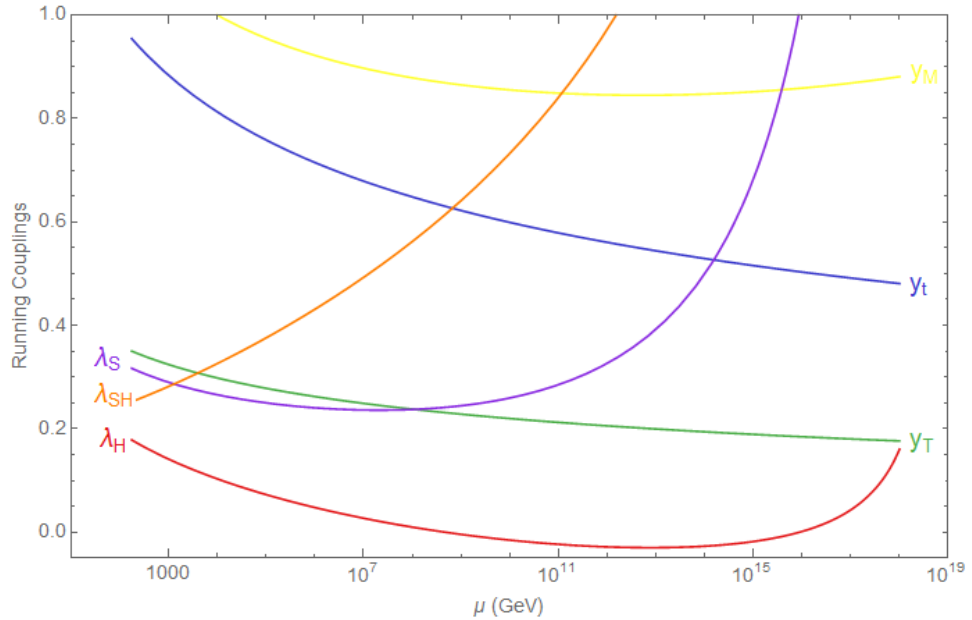

Figure 5.3: The RGE running of the Yukawa and scalar couplings for the vectorlike fermion model. We have set $m_T = 0.8$ TeV, $m_S = 0.8$ TeV, $\sin\theta_L = 0.08$, $\sin\phi = 0.1$, $u = 1$ TeV, and the starting point is at $\mu_0 = m_t$.

Just as in the previous model, we require

$$\lambda_H > 0, \qquad 0 < \lambda_S < 4\pi, \qquad |\lambda_{SH}| < 4\pi \tag{84}$$

for increasing field values in order to ensure a positive potential and thus a stable vacuum.

We may then study the allowed parameter values corresponding to each hypothetical particle. In order to achieve this, we perform a scan over random values of m_S and m_T between

45

Figure 5.4: The RGE running of the Yukawa and scalar couplings for the vectorlike fermion model. We have set $m_T = 0.8$ TeV, $m_S = 1$ TeV, $\sin\theta_L = 0.08$, $\sin\phi = 0.1$, $u = 2$ TeV, and the starting point is at $\mu_0 = m_t$.
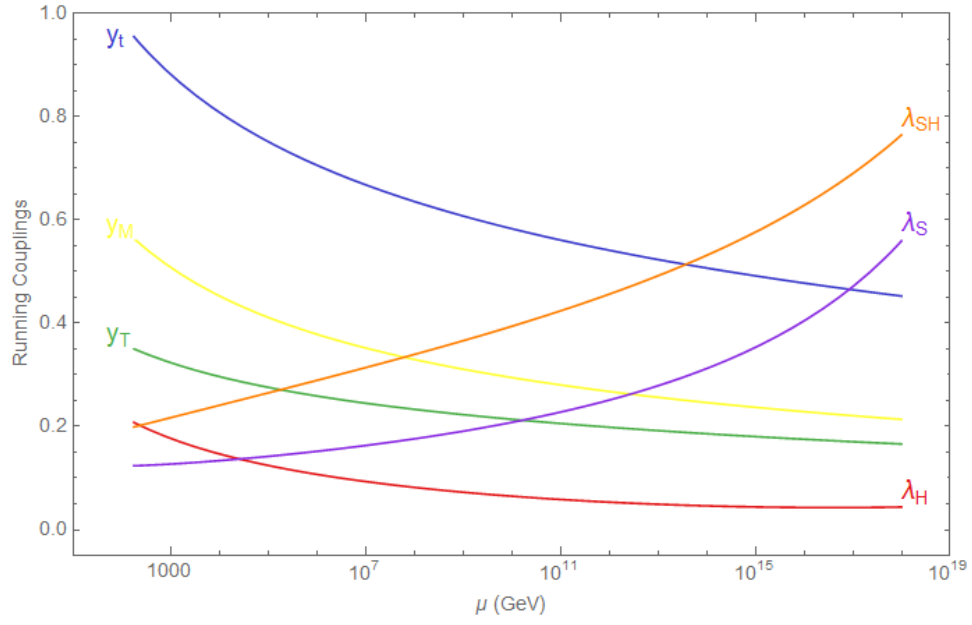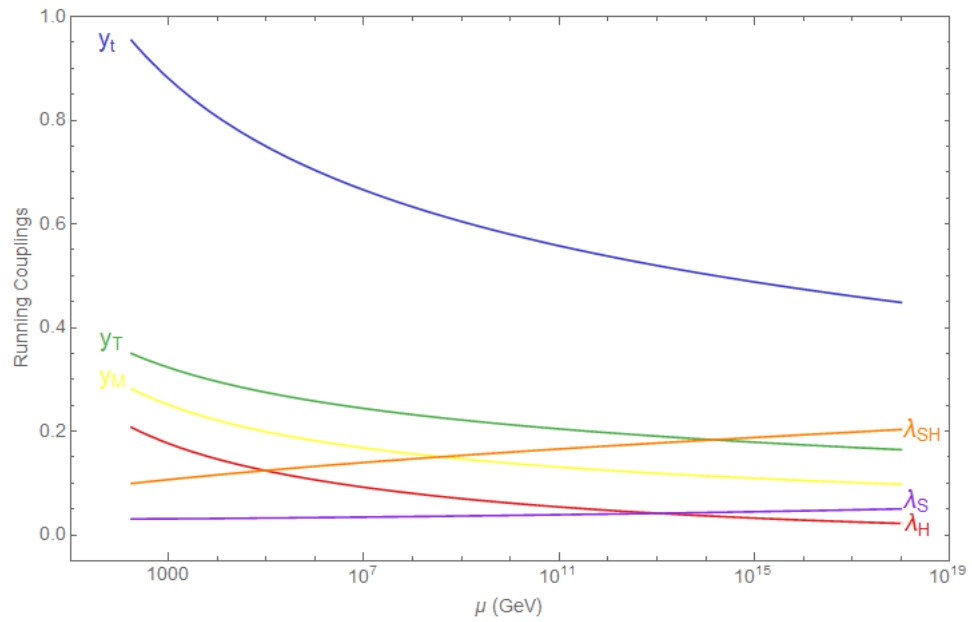

Figure 5.5: The RGE running of the Yukawa and scalar couplings for the vectorlike fermion model. We have set $m_T = 0.8$ TeV, $m_S = 1$ TeV, $\sin\theta_L = 0.08$, $\sin\phi = 0.1$, $u = 4$ TeV, and the starting point is at $\mu_0 = m_t$.

46

300 and 2200 GeV, and $\sin\phi$ and $\sin\theta_L$ between -1 and 1. Parameter values satisfying the conditions outlined in Eq.(84) are conserved and plotted below, while those that do not are discarded. The allowed values of m_S are then plotted against the allowed values of $\sin\phi$ in Figure 5.6 for different vacuum expectation values u, providing us with an illustration of the possible quantitative properties of the scalar boson in this model. Similarly, the allowed values of m_T are plotted against those of $\sin\theta_L$ in Figure 5.7, giving us insight about the extra fermion in this model.

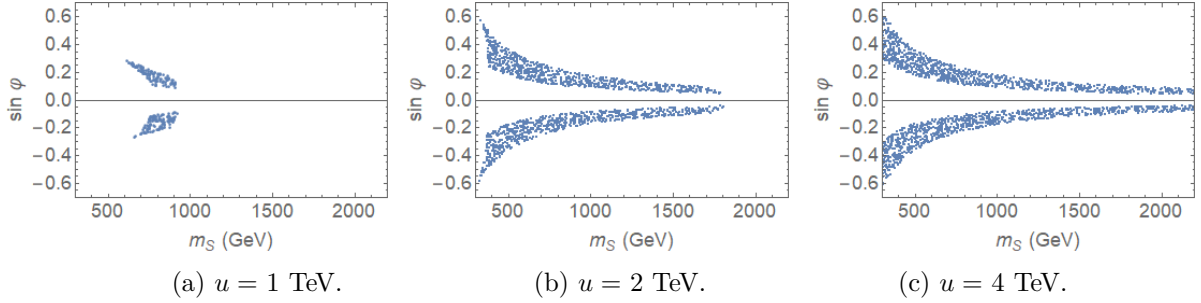(a) $u = 1$ TeV.　　　　(b) $u = 2$ TeV.　　　　(c) $u = 4$ TeV.

Figure 5.6: The allowed parameter space for the scalar boson mass and mixing angle in the additional fermion two-Higgs model for different vacuum expectation values.

(a) $u = 1$ TeV.　　　　(b) $u = 2$ TeV.　　　　(c) $u = 4$ TeV.
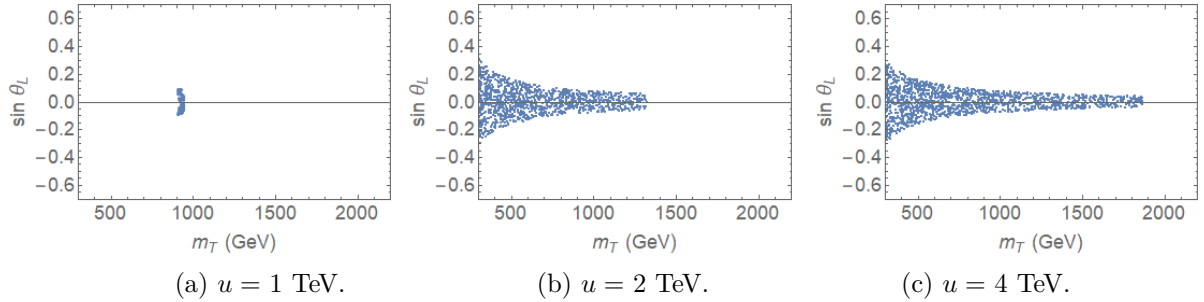
Figure 5.7: The allowed parameter space for the vectorlike fermion mass and mixing angle in the additional fermion and scalar model for different vacuum expectation values.

We remark from Figure 5.6 that just as in the SM extension containing only an extra scalar boson, considered in the previous chapter, there is necessarily mass mixing between the two scalar bosons. However, when we consider the fermions t and T, we conclude that the mixing between the two must be minimal, or possibly even nonexistent, as evidenced by the cluster of allowed values near the zero mixing axis in Figure 5.7.

Chapter 6

Vacuum stability in quark doublet two-Higgs models

6.1 Vacuum stability in a $Y = \frac{1}{6}$ quark doublet two-Higgs model

In this chapter, we explore yet another extension of the SM containing again the extra scalar boson, however we now replace the one extra fermion of the previous model with a fermion doublet, or generation. In the SM, the quarks are separated into three pairs called "generations", separated by their masses. Like these SM doublets, the extra doublet considered in this extension will consist of a quark with a charge of $+2/3$ and the other, a charge of $-1/3$. We will call these quarks T and B respectively, as they can be thought of simply as heavier top and bottom quarks, but with same left-handed and right-handed interactions.

The Yukawa couplings involving this vectorlike fermion doublet $\psi = \begin{pmatrix} T \\ B \end{pmatrix}$ and the third

generation quarks $Q_L = \begin{pmatrix} \tau_L \\ b_L \end{pmatrix}$, τ_R and b_R provide the Lagrangian with the following terms:

$$-\mathcal{L}_{Yukawa} = \frac{y_M}{\sqrt{2}}\chi\bar{\psi}_L\psi_R + \frac{\lambda_T}{\sqrt{2}}\chi\bar{Q}_L\psi_R + y_t\bar{Q}_L\tilde{H}\tau_R + y_b\bar{Q}_L\tilde{H}b_R + y_T\bar{\psi}_L\tilde{H}\tau_R + y_B\bar{\psi}_L\tilde{H}b_R + \text{h.c.}$$
(85)

and the additional Dirac mass term in Eq.(65) remains unchanged.

We begin by considering how an extra quark generation will affect the gauge couplings. Since this quark doublet will interact with the gauge bosons (in other words, it will experience the fundamental forces), it will add contributions to these gauge coupling parameters. The corresponding gauge coupling RGEs are

$$\frac{dg_1^2}{d\ln\mu^2} = \frac{g_1^4}{(4\pi)^2}\left(\frac{41}{10} + \frac{2}{15}\right),$$
(86)

$$\frac{dg_2^2}{d\ln\mu^2} = \frac{g_2^4}{(4\pi)^2}\left(-\frac{19}{6} + 2\right),$$
(87)

$$\frac{dg_3^2}{d\ln\mu^2} = \frac{g_3^4}{(4\pi)^2}\left(-7 + \frac{4}{3}\right).$$
(88)

Again, the first terms represent the SM RGEs, while the second terms are the contributions from the extra generation considered in this model.

As for the Yukawa couplings, we now must consider the top Yukawa coupling y_t (which is modified by the presence of the additional doublet), as well as the new Yukawa couplings, y_T and y_B. In addition, for the sake of simplicity, we will assume that the new fermion doublet interacts with the new scalar together as a single entity and call this coupling y_M. Before presenting the running coupling parameters, let us first establish the Yukawa couplings at low energy scales, which will serve as initial conditions for the running RGEs. Just as in the previous model, we do this by diagonlizing the mass matrices. The low energy scale Yukawa couplings are obtained in the same way as the previous model. In fact, the mass mixing between b and B is exactly identical to that between t and T, with $t \to b$, $T \to B$

and $\theta_{L,R} \to \beta_{L,R}$, yielding

$$y_t(\mu_0) = \frac{\sqrt{2}m_t}{v} \frac{1}{\sqrt{\cos^2 \theta_L + x_t^2 \sin^2 \theta_L}}, \tag{89}$$

$$y_T(\mu_0) = \frac{\sqrt{2}m_T}{v} \frac{\sin \theta_L \cos \theta_L (1 - x_t^2)}{\sqrt{\cos^2 \theta_L + x_t^2 \sin^2 \theta_L}}, \tag{90}$$

$$y_B(\mu_0) = \frac{\sqrt{2}m_B}{v} \frac{\sin \beta_L \cos \beta (1 - x_b^2)}{\sqrt{\cos^2 \beta_L + x_b^2 \sin^2 \beta_L}}, \tag{91}$$

$$y_M(\mu_0) = \frac{m_T + m_B}{\sqrt{2}u} \sqrt{\cos^2 \theta_L + x_t^2 \sin^2 \theta_L}. \tag{92}$$

Recall that x_t is the ratio of the top mass and the T mass. Similarly, $x_b = m_b/m_B$, and θ_L is the mass mixing angle between t and T, while β_L is the mass mixing angle between b and B. The above-noted initial conditions are again evaluated at $\mu_0 = m_t$.

The RGEs for the running of these Yukawa couplings are as follows:

$$\frac{dy_t^2}{d\ln\mu^2} = \frac{y_t^2}{(4\pi)^2} \left(\frac{9y_t^2}{2} + \frac{9y_T^2}{2} + \frac{3y_B^2}{2} + \frac{y_M^2}{4} - \frac{17g_1^2}{20} - \frac{9g_2^2}{4} - 8g_3^2 \right), \tag{93}$$

$$\frac{dy_T^2}{d\ln\mu^2} = \frac{y_T^2}{(4\pi)^2} \left(\frac{9y_t^2}{2} + \frac{9y_T^2}{2} + \frac{3y_B^2}{2} + \frac{y_M^2}{4} - \frac{17g_1^2}{20} - \frac{9g_2^2}{4} - 8g_3^2 \right), \tag{94}$$

$$\frac{dy_B^2}{d\ln\mu^2} = \frac{y_B^2}{(4\pi)^2} \left(\frac{3y_t^2}{2} + \frac{3y_T^2}{2} + \frac{9y_B^2}{2} + \frac{y_M^2}{4} - \frac{g_1^2}{4} - \frac{9g_2^2}{4} - 8g_3^2 \right), \tag{95}$$

$$\frac{dy_M^2}{d\ln\mu^2} = \frac{y_M^2}{(4\pi)^2} \left(y_T^2 + y_B^2 + \frac{9y_M^2}{2} - \frac{8g_1^2}{5} - 8g_3^2 \right). \tag{96}$$

Now, directing our attention to the final possible type of coupling, namely the Higgs sector couplings, we find that the initial conditions evaluated at $\mu_0 = m_t$ are of course identical to those presented in the previous model in Eqs. (48)-(50), since couplings are considered constant at such small energy scales.

However, with the added possible interactions arising from the presence of the new fermion doublet, more loop contributions must be considered at higher energies, and the RGEs must be modified to reflect these possible interactions. As we restrict the new scalar boson's

50

interactions to the Higgs boson and the additional quark doublet to be unique, the Higgs-like scalar quartic coupling RGE will not contain any explicit dependence on any of the individual quarks (t, T, and B), but rather only with the Higgs sector.

The Higgs sector RGEs for this model are

$$
\begin{aligned}
\frac{d\lambda_H}{d\ln\mu^2} &= \frac{1}{(4\pi)^2}\left[\lambda_H\left(12\lambda_H + 6y_t^2 + 6y_T^2 + 6y_B^2 - \frac{9g_1^2}{10} - \frac{9g_2^2}{2}\right)\right. \\
&\left. + \frac{\lambda_{SH}^2}{4} - 3y_t^4 - 3y_T^4 - 3y_B^4 - 6y_t^2 y_T^2 + \frac{27g_1^4}{100} + \frac{9g_2^4}{16} + \frac{9g_1^2 g_2^2}{40}\right], \quad (97)
\end{aligned}
$$

$$
\frac{d\lambda_S}{d\ln\mu^2} = \frac{1}{(4\pi)^2}\left(9\lambda_S^2 + \lambda_{SH}^2 + 6y_M^2\lambda_S - 6y_M^4\right), \quad (98)
$$

$$
\begin{aligned}
\frac{d\lambda_{SH}}{d\ln\mu^2} &= \frac{1}{(4\pi)^2}\left[\lambda_{SH}\left(6\lambda_H + 3\lambda_S + 2\lambda_{SH} + 3y_t^2 + 3y_T^2 + 3y_B^2 + 6y_M^2 - \frac{9g_1^2}{20} - \frac{9g_2^2}{4}\right)\right. \\
&\left. - 6y_T^2 y_M^2 - 6y_B^2 y_M^2\right]. \quad (99)
\end{aligned}
$$

Figure 6.1 illustrates the running of all the relevant coupling parameters presented in this model for a typical set of parameter values. As required, all of the Higgs sector couplings remain positive up to Planck scale (10^{18} GeV). We notice a trend with respect to the previous models presented in this thesis; the Yukawa couplings are generally affected negatively by the added loops at higher energy scales, while the Higgs sector couplings are generally affected positively (they tend to increase with increasing energy). The obvious exception here is the Higgs coupling, which strays dangerously close to zero at high energy scales. This, of course, depends on the parameter values chosen, however this general trend serves us well as this allows us to impose limits on these parameter values.

This leads us to wonder about the allowed masses and mass mixing angles of the hypothetical scalar boson and fermion doublet that will yield a positive Higgs coupling and thus a stable Higgs vacuum (i.e. a successful Standard Model) up to Planck scale. To this end, we perform a scan over a broad parameter region just as we did in the previous models and illustrate the successful parameter value combinations.
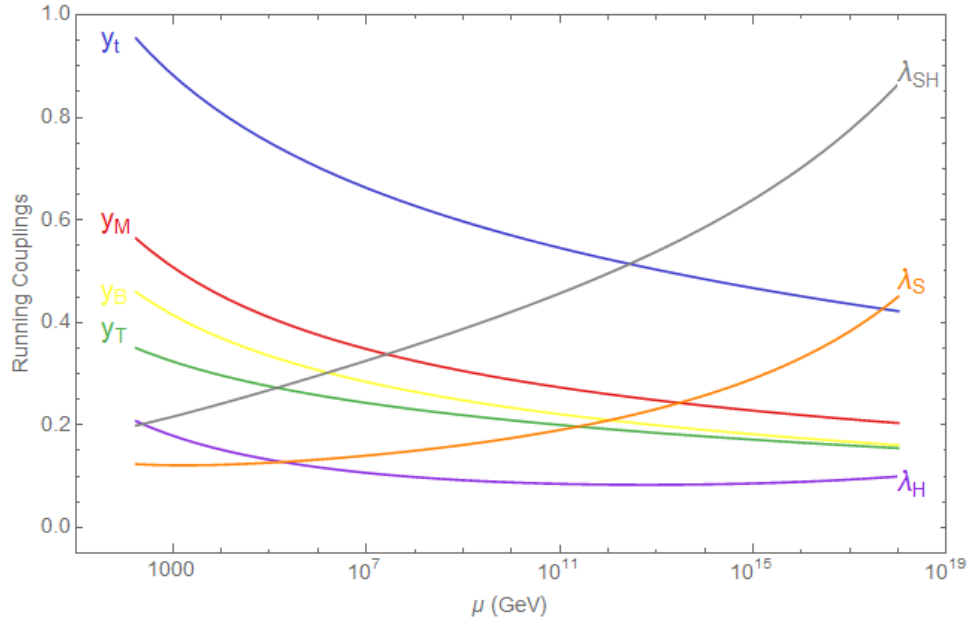
Figure 6.1: The RGE running of the Yukawa and Higgs sector couplings for the fermion doublet model. We have set $m_T = 0.8\text{TeV}$, $m_B = 1$ TeV, $m_S = 1$ TeV, $\sin\theta_L = \sin\beta_L = 0.08$, $\sin\phi = 0.1$, $u = 2$ TeV, and the starting point is at $\mu_0 = m_t$.

Figure 6.2 illustrates the permitted mass and mixing angle values for the scalar boson in this model for a few different scalar vacuum expectation values u. Figures 6.3 and 6.4 illustrate the allowed masses and mixing angles for the fermion doublet T and B, respectively.

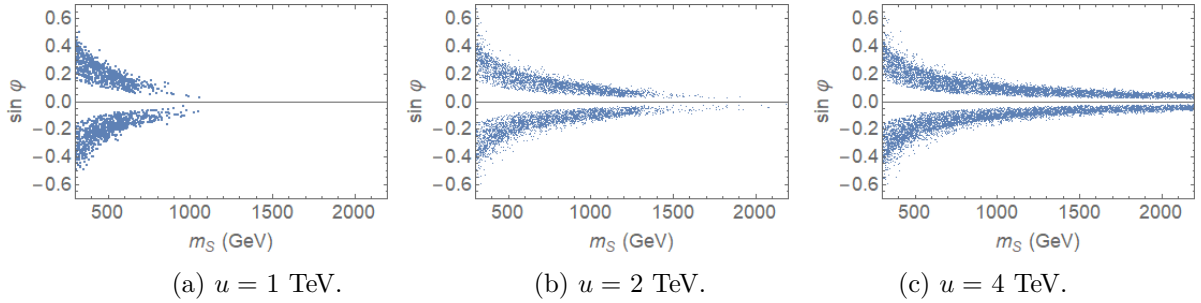(a) $u = 1$ TeV. (b) $u = 2$ TeV. (c) $u = 4$ TeV.

Figure 6.2: The allowed parameter space for the scalar boson mass and mixing angle in the additional fermion doublet model for different vacuum expectation values.
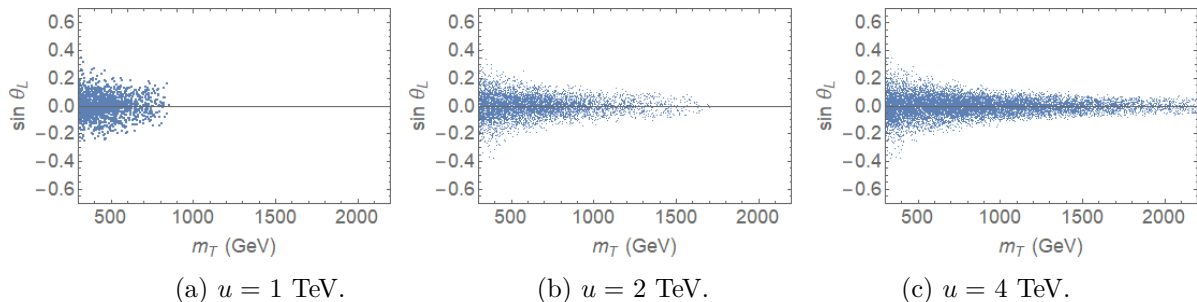
(a) $u = 1$ TeV.   (b) $u = 2$ TeV.   (c) $u = 4$ TeV.

Figure 6.3: The allowed parameter space for the T fermion mass and mixing angle in the additional fermion doublet model for different vacuum expectation values.

We see that the allowed parameter spaces in this additional fermion doublet model look similar to those obtained in the additional fermion singlet model. As expected from previous observations, the permitted parameter spaces appear very similar for different scalar VEVs u, with the larger VEVs merely allowing for larger masses. Just as in the fermion singlet model, there is necessarily a mass mixing between the two Higgs sector scalars, illustrated by the empty space along the central axis in Figure 6.2, while there is little to no mass mixing between the fermion doublets (t,b) and (T,B).

(a) $u = 1$ TeV.   (b) $u = 2$ TeV.   (c) $u = 4$ TeV.

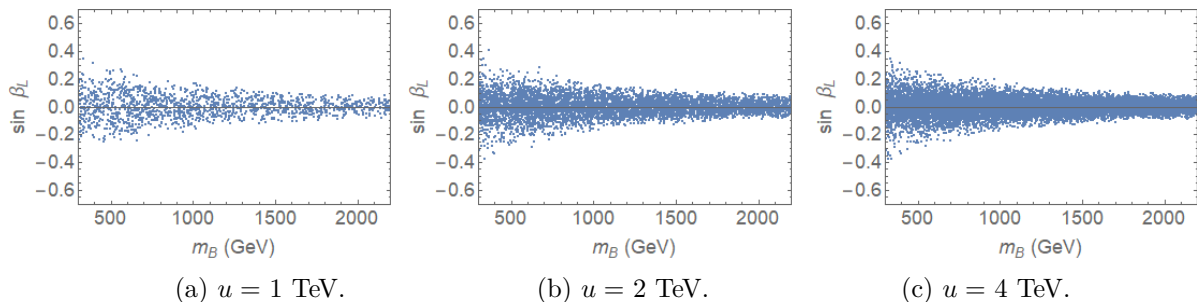Figure 6.4: The allowed parameter space for the B fermion mass and mixing angle in the additional fermion doublet model for different vacuum expectation values.

6.2   Vacuum stability in a $Y = \frac{7}{6}$ quark doublet in the two-Higgs model

Finally, the final model we will consider, much like the previous model, contains a fourth quark doublet, however rather than this quark doublet containing electric charges of $+2/3$

and $-1/3$ like the three existing quark generations, we will consider a fourth generation in which the quarks have electric charges of $+2/3$ and $+5/3$ (which we will label T and X, respectively). In other words, we will entertain the possibility of a $Y = 7/6$ doublet, in contrast with the three familiar generations containing each a positive and negative quark pair. The motivation for this is twofold: firstly, purely for investigating new possibilities consistent with extra symmetries and their implications, and secondly, because it is allowed by the observed symmetries governing electric charge (QED) and colour (QCD), and interacts with the gauge bosons of the SM.

All stable particles observed experimentally possess electric charges which are integer multiples of the electron's charge. Only quarks possess fractional charges, however quarks cannot be observed directly on their own, as this is forbidden by chromodynamics. We know from chromodynamics that quarks can only form "colourless" combinations. As we have seen, this leaves room for triplets of quarks or anti-quarks (baryons), as well as quark/anti-quark pairs (mesons). Verifying that such combinations always yield an integer charge value is a simple exercise in arithmetic. The six quarks within the SM are known to have charges of $+2/3$ and $-1/3$—any combination of three of which will yield an integer value. The same applies for any set of three anti-quarks, which simply have opposite charges of $-2/3$ and $+1/3$. Likewise, any pairing of one quark and one anti-quark results in an integer charge meson.

Upon introducing the aforementioned new quark generation, the possible quark and anti-quark charges become $+5/3$, $+2/3$, $-1/3$, and $-5/3$, $-2/3$, $+1/3$, respectively. It is easy to check that again, any baryon or meson combination yields an integer charge result.

The Yukawa couplings involving this vectorlike fermion doublet $\psi = \begin{pmatrix} X \\ T \end{pmatrix}$ and the top quark τ provide the Lagrangian with the following terms:

$$-\mathcal{L}_{Yukawa} = \frac{y_M}{\sqrt{2}} \chi \bar{\psi}_L \psi_R + \frac{\lambda_T}{\sqrt{2}} \chi \bar{Q}_L \psi_R + y_t \bar{Q}_L \tilde{H} \tau_R + y_T \bar{\psi}_L \tilde{H} \tau_R + \text{h.c.} \qquad (100)$$

And, again, the additional Dirac mass term in Eq.(65) remains unchanged.

We now turn our attention to the RGEs and Higgs bound for this model. Beginning with the foundations, we consider how the running of the gauge couplings will change. Note that the gauge coupling runnings will remain mostly identical to those in the traditional doublet model, as both models contain the same number of fermions. However, the only gauge coupling which must be modified is the U(1) gauge behind the QED eleric charges, which is to be expected given the new charge of 5/3. The gauge coupling RGEs are

$$\frac{dg_1^2}{d\ln\mu^2} = \frac{g_1^4}{(4\pi)^2}\left(\frac{41}{10} + \frac{98}{15}\right), \tag{101}$$

$$\frac{dg_2^2}{d\ln\mu^2} = \frac{g_2^4}{(4\pi)^2}\left(-\frac{19}{6} + 2\right), \tag{102}$$

$$\frac{dg_3^2}{d\ln\mu^2} = \frac{g_3^4}{(4\pi)^2}\left(-7 + \frac{4}{3}\right). \tag{103}$$

We now implement the Yukawa Higgs couplings. Beginning at the low energy limit, we can extrapolate the Yukawa coupling constants from the single fermion model in the same manner as we did for the previous fermion doublet model. The only significant change here is that the quark that we label X—bearing the charge of +5/3—will not mix with another quark, as no other quarks have this electric charge, and the electroweak gauge requires this symmetry to be obeyed with respect to mass mixing. We will, however, continue to allow for mass mixing between the T and top quarks. The resulting low energy limit Yukawa couplings, or Yukawa RGE initial conditions, are as follows:

$$y_t(\mu_0) \;\; = \;\; \frac{\sqrt{2}m_t}{v}\frac{1}{\sqrt{\cos^2\theta_L + x_t^2 \sin^2\theta_L}}, \tag{104}$$

$$y_X(\mu_0) \;\; = \;\; \frac{\sqrt{2}m_X}{v}, \tag{105}$$

$$y_T(\mu_0) \;\; = \;\; \frac{\sqrt{2}m_T}{v}\frac{\sin\theta_L \cos\theta_L (1 - x_t^2)}{\sqrt{\cos^2\theta_L + x_t^2 \sin^2\theta_L}}, \tag{106}$$

$$y_M(\mu_0) \;\; = \;\; \frac{m_X + m_T}{\sqrt{2}u}\sqrt{\cos^2\theta_L + x_t^2 \sin^2\theta_L}. \tag{107}$$

As for the Yukawa RGEs themselves, they too are modified slightly, becoming

$$\frac{dy_t^2}{d\ln\mu^2} \;\; = \;\; \frac{y_t^2}{(4\pi)^2}\left(\frac{9y_t^2}{2} + \frac{9y_X^2}{2} + \frac{3y_T^2}{2} - \frac{17g_1^2}{20} - \frac{9g_2^2}{4} - 8g_3^2\right), \tag{108}$$

$$\frac{dy_X^2}{d\ln\mu^2} \;\; = \;\; \frac{y_X^2}{(4\pi)^2}\left(\frac{9y_t^2}{2} + \frac{9y_X^2}{2} + \frac{3y_T^2}{2} + \frac{y_M^2}{4} - 2g_1^2 - \frac{9g_2^2}{4} - 8g_3^2\right), \tag{109}$$

$$\frac{dy_T^2}{d\ln\mu^2} \;\; = \;\; \frac{y_T^2}{(4\pi)^2}\left(\frac{3y_t^2}{2} + \frac{3y_X^2}{2} + \frac{9y_T^2}{2} + \frac{y_M^2}{4} - \frac{17g_1^2}{20} - \frac{9g_2^2}{4} - 8g_3^2\right), \tag{110}$$

$$\frac{dy_M^2}{d\ln\mu^2} \;\; = \;\; \frac{y_M^2}{(4\pi)^2}\left(y_X^2 + y_T^2 + \frac{9y_M^2}{2} - \frac{8g_1^2}{5} - 8g_3^2\right). \tag{111}$$

The most notable difference here compared to the generic fourth quark doublet model is the lack of y_M dependence in Eq.(108): The break in electroweak symmetry, that is to say, the shifted electric charges, results in the decoupling of the Yukawa couplings of the third quark generation with that of this symmetry-breaking fourth generation.

Finally, we require the Higgs sector RGEs. Just as with the previous extra doublet model, we will limit the new scalar boson's interactions to involve strictly the Higgs as well as the new doublet, excluding all individual quarks. The scalar self-coupling λ_S then depends again only on y_M and not the individual quark Yukawa couplings.

The Higgs sector RGEs for this model are similar to those presented in the previous doublet model, only with the B quark replaced by the X quark. The complete array of Higgs sector

RGEs is then

$$
\frac{d\lambda_H}{d\ln\mu^2} = \frac{1}{(4\pi)^2}\left[\lambda_H\left(12\lambda_H + 6y_t^2 + 6y_X^2 + 6y_T^2 - \frac{9g_1^2}{10} - \frac{9g_2^2}{2}\right)\right.
$$
$$
\left. + \frac{\lambda_{SH}^2}{4} - 3y_t^4 - 3y_X^4 - 3y_T^4 - 6y_t^2 y_T^2 + \frac{27g_1^4}{100} + \frac{9g_2^4}{16} + \frac{9g_1^2 g_2^2}{40}\right], \tag{112}
$$

$$
\frac{d\lambda_S}{d\ln\mu^2} = \frac{1}{(4\pi)^2}\left(9\lambda_S^2 + \lambda_{SH}^2 + 6y_M^2\lambda_S - 6y_M^4\right), \tag{113}
$$

$$
\frac{d\lambda_{SH}}{d\ln\mu^2} = \frac{1}{(4\pi)^2}\left[\lambda_{SH}\left(6\lambda_H + 3\lambda_S + 2\lambda_{SH} + 3y_t^2 + 3y_X^2 + 3y_T^2 + 6y_M^2 - \frac{9g_1^2}{20} - \frac{9g_2^2}{4}\right)\right.
$$
$$
\left. - 6y_X^2 y_M^2 - 6y_T^2 y_M^2\right]. \tag{114}
$$

Having established all of the necessary running couplings, we now have a complete picture of the coupling parameters at all energy scales up to Planck scale, as illustrated in Figure 6.5.
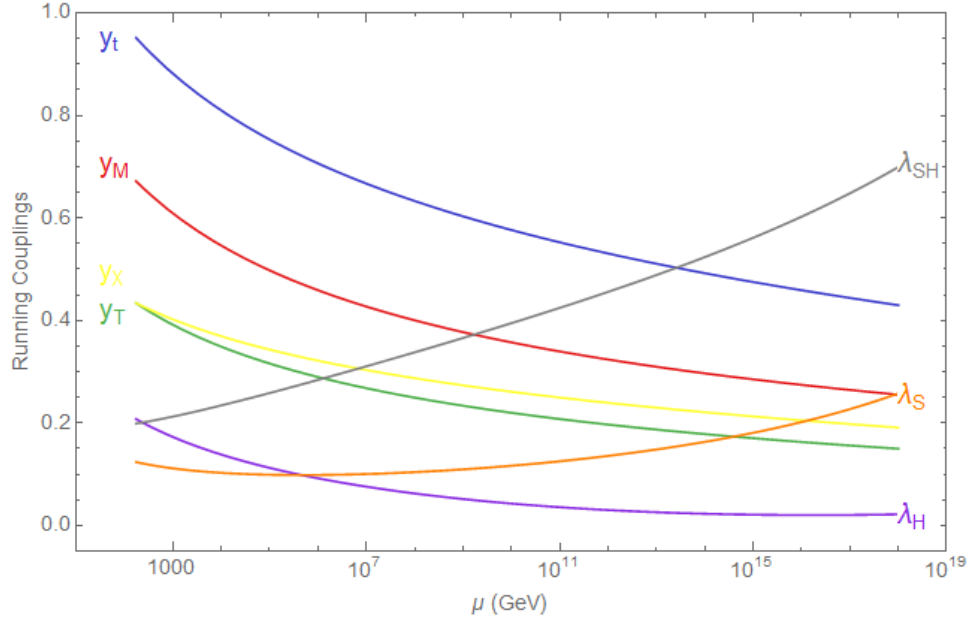

Figure 6.5: The RGE running of the Yukawa and Higgs sector couplings for the $Y = 7/6$ fermion doublet model. We have set $m_X = m_T = 0.8$ TeV, $m_S = 1$ TeV, $\sin\theta_L = \sin\phi = 0.1$, $u = 2$ TeV, and the starting point is at $\mu_0 = m_t$.

We see again that the fermion Yukawa couplings tend to decrease with increasing energy, while the scalar bosonic couplings tend to increase. This loosely explains why the addition of

extra scalar bosons to the SM helps maintain a positive Higgs self-coupling at larger energy scales, while the addition of extra fermions only aids in dropping it further. The Higgs self-coupling, which dips dangerously close to zero, is weighed down by the large number of fermions that it interacts with. This is the vacuum stability bound that we are particularly interested in; for the conditions under which the quartic coupling remains positive up to Planck scale are somewhat limited and thus very telling. The quartic coupling of the new scalar does not exhibit a behavior of lying close to the origin due to limiting its fermionic interactions. This choice, while admittedly somewhat arbitrary, does not impede the goal of studying the Higgs vacuum stability bound specifically. We are less interested in the new scalar vacuum stability bound since we can only speculate about the mass and VEV of such a field, and thus we cannot obtain much concrete information from a detailed study of its vacuum stability bound.

We will now look at what the positive quartic coupling, or vacuum stability, requirement implies about the model's parameters.

Figure 6.6 illustrates the allowed parameter space for the new scalar boson's mass and mass mixing angle with the Higgs for different VEVs. We see that the parameter space is quite similar to that of the regular additional doublet model, with only a reduced maximum mass. This implies that should this model be a reflection of extra particles, as we reach higher energies and masses, the mass cutoff occurs sooner than in the regular doublet model. In other words, this model is experimentally more restricted and easier to rule out. This model is of course less likely intuitively and theoretically as well, given our desire for symmetry and the lack of such a generation in the SM to date.

In Figure 6.7, we examine the allowed masses of the X & T quark doublet (recall that there is no mass mixing associated with the X quark). We see that both particles have an allowed mass of approximately 900–1040 GeV.

Finally, in Figure 6.8, we study the allowed parameter space for the T quark mass and mass mixing angle with the top quark for different VEVs. We again confirm that the mass of the

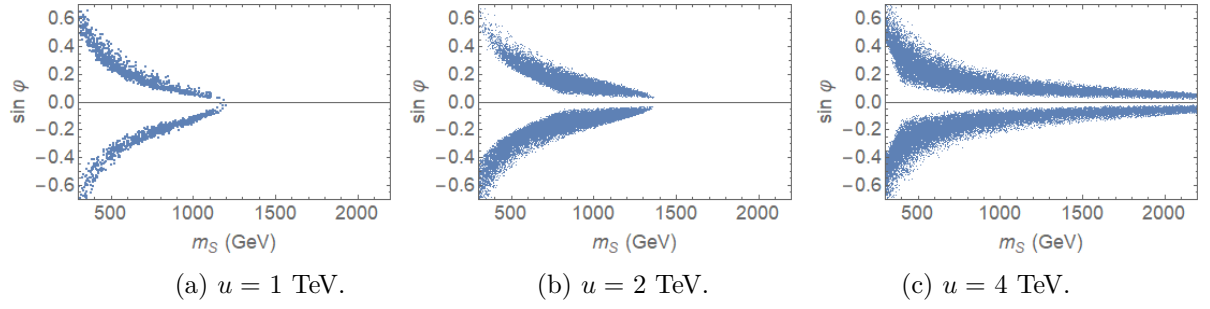(a) $u = 1$ TeV. (b) $u = 2$ TeV. (c) $u = 4$ TeV.

Figure 6.6: The allowed parameter space for the scalar boson mass and mixing angle in the positively charged quark doublet model for different vacuum expectation values.

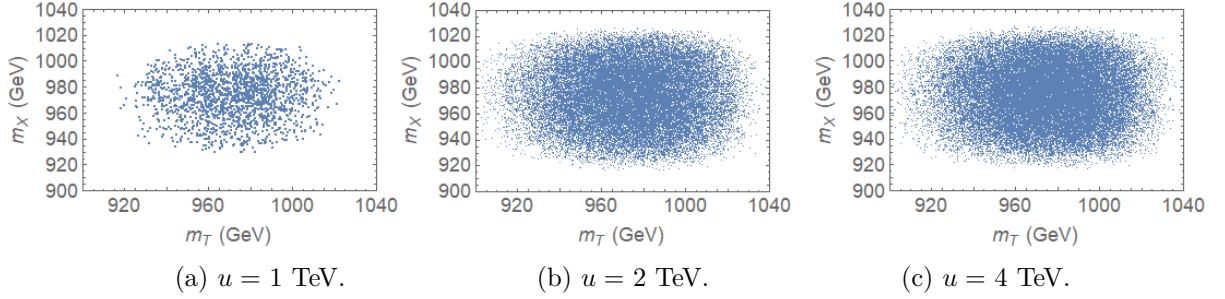(a) $u = 1$ TeV. (b) $u = 2$ TeV. (c) $u = 4$ TeV.

Figure 6.7: The allowed parameter space for the X and T quark masses in the $Y = 7/6$ quark doublet model for different vacuum expectation values.

T quark is around 900–1000 GeV, and interestingly, we see that with a low VEV, there is forced mass mixing between T and t, however there is more freedom for larger VEVs.
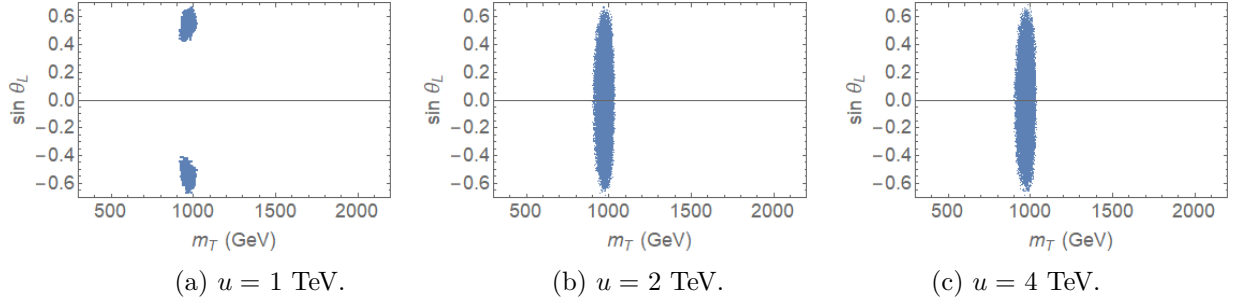

(a) $u = 1$ TeV. (b) $u = 2$ TeV. (c) $u = 4$ TeV.

Figure 6.8: The allowed parameter space for the T fermion mass and mixing angle in the $Y = 7/6$ fermion doublet model for different vacuum expectation values.

Chapter 7

Conclusions

At observable energies, The Standard Model is a very successful theory, as it precisely
describes the matter and interactions known to us. The experimental discovery of the
Higgs boson in 2012 was at once a major affirmation of the theory and a glaring problem.
On one hand, its existence was a major theoretical necessity of the SM, and so its discovery
after a forty-year search suggests that the theory is correct. However, on the other hand, its
mass of 125 GeV is troublesome, as this implies one of three things: firstly, that the Higgs is
trapped in a false vacuum, and that a sufficiently high-energy event could, in principle, cause
it to decay and move into a true vacuum state. This would have an effect analogous to a
superheated fluid, in that bubbles of true vacuum would form, and then expand, incinerating
the universe as it decays its false vacuum at the speed of light. The second possible result is
that the SM simply is not valid up to Planck scale, or Unification scale. This implies that
the SM is merely an approximation of a more fundamental theory, much like Newtonian
mechanics is a good low-energy approximation of general relativity. Finally, the third and
simplest explanation lies in SM extensions, taking the form of any of the models considered
in this thesis or any of the infinite number of other possible arrangements. This vacuum
stability solution is preferable to the previous two because it does not require a great amount
of reshaping of our understanding of particle physics. In fact, given the large number of

elementary particles discovered to date and how spaced out these discoveries have been over time, with the Higgs having been discovered only a few short years ago, the prospect of new particles does not demand a great stretch of the imagination. Plus, this simple explanation is a great candidate for explaining other missing gaps in the SM, especially dark matter.

In regards to vacuum stabilizing, in this thesis we have proposed a number of simple extensions which stabilize the Higgs vacuum, by adding another heavier Higgs-like scalar boson in each case. It has been tested and verified that additional fermions only exacerbate the stability problem, however additional scalar bosons offer a very easy fix, even when combined with these problematic fermions. We have studied the limits imposed by the vacuum stability condition on the masses and mass mixing angles of the elementary particles in each model. We observe that for the SM presumed valid up to Planck scale, a lower limit of approximately 135 GeV is imposed on the Higgs mass, contradicting the confirmed experimental value of 125 GeV. In SM extensions containing additional scalar bosons and fermions, this Higgs mass is acceptable provided there is another scalar boson which lightens the load of the Higgs, so to speak. Any additional quarks are required to mix with previous generations, as is the case for the SM quarks. The additional Higgs-like boson, however, is required to have little or no mixing with the Higgs.

There exist other motivations independent of vacuum stability to extend the SM Higgs sectorâĂŤextra scalar bosons are often introduced as dark matter candidates [15, 16, 27, 22, 14], and the convergence of the electromagnetic, weak and strong coupling constants at high energies can be achieved through additional Higgs representations [55, 56].

The models introduced in this thesis, while focused on the extension of the Higgs sector, simultaneously explore additional fermionic particles, for the SM can be extended by both scalar and fermionic fields. However, unlike the chiral SM fermions, all of the fermionic extensions presented in these models are vectorlike fermions. This is because extra chiral generations are ruled out by the experimental data with respect to cross-section and diphoton decay of the SM Higgs boson [57]. The addition of non-chiral fermionic representations,

on the other hand, is much less constrained.

In this thesis, we have reproduced results presented in the literature for the SM, the two-Higgs model and the vectorlike fermion two-Higgs model. Furthermore, we have presented a more thorough analysis of these models by producing graphs of the running couplings and the mass bounds for the two-Higgs model, as well as additional graphs for the vectorlike fermion model to illustrate the running couplings for $u = 1$ TeV and $u = 4$ TeV. We then diverged from the literature in order to analyze the implications of vacuum stability in the $Y = 1/6$ and $Y = 7/6$ fermion doublet models.

As evidenced in this thesis, minimal SM extensions involving a second scalar boson very elegantly unravel the glaring problem of vacuum instability in the SM. However, such speculations can only be confirmed by experimental observations, such as high-energy collisions in particle accelerators, like CERN's Large Hadron Collider. With higher energies, it is possible to produce particles bearing larger masses in collision events (due to Einstein's mass-energy equivalence). With the Higgs being discovered only during the last run, it is not unreasonable to expect another, more massive, scalar boson to emerge from even higher-energy collisions, for although the Standard Model predicted the existence of at least one scalar boson, in extended models more bosons are predicted. No matter the types or masses of particles that might emerge from these experiments, however, we can be sure that they hold the promise of answering our long-standing questions about vacuum stability, dark matter and perhaps more.

Appendix A

Mathematica computations

Below is an example of the computations performed using Mathematica for the $Y = 1/6$ quark doublet two-Higgs model with $u = 2$ TeV.

Constants

```
mt = 174; mb = 4.18; mZ = 91.188; mH = 125;

v = 246.22; w = 2000; Gu = 0.0000116635;

xt[mT_] := mt / mT; xb[mB_] := mb / mB;

cf[sf_] := Sqrt[1 - sf^2]; cl[sl_] := Sqrt[1 - sl^2];

a = 1 / 127.926; as = 0.118; sw = 0.2312; cw = 1 - sw;

u0 = mt;

Nc = 3; Cf = (Nc^2 - 1) / (2 * Nc); Qt = 2 / 3;
```

Gauge couplings

```
g10 = Sqrt[4 * Pi * a]; g20 = Sqrt[g10^2 / sw - g10^2]; g30 := Sqrt[4 * Pi * as];

g1[u_] := (1 / g10^2 - 1 / (4 * Pi)^2 * (41 / 10 + 2 / 15) * (Log[u^2] - Log[u0^2]))^(-1 / 2);

g2[u_] := (1 / g20^2 - 1 / (4 * Pi)^2 * (-19 / 6 + 2) * (Log[u^2] - Log[u0^2]))^(-1 / 2);

g3[u_] := (1 / g30^2 - 1 / (4 * Pi)^2 * (-7 + 4 / 3) * (Log[u^2] - Log[u0^2]))^(-1 / 2);
```

Electroweak radiative correction term

```
dQCD[u_] := Cf * as / (4 * Pi) * (3 * Log[mt^2 / u^2] - 4);

dQED[u_] := Qt^2 * a / (4 * Pi) * (3 * Log[mt^2 / u^2] - 4);

dW[u_] := Gu * mt^2 / (8 * Pi^2 * Sqrt[2]) * (- (Nc + 3 / 2) * Log[mt^2 / u^2] + Nc / 2 + 4 - 2 * Pi * mH / mt);

df[u_] := dW[u] + dQED[u] + dQCD[u];
```

Yukawa couplings

```
yM0[mT_, mB_, sl_] := Sqrt[2] * ((mT + mB) / 2) / w * Sqrt[cl[sl]^2 + xt[mT]^2 * sl^2];

yT0[mT_, sl_] := Sqrt[2] * mT / v * sl * cl[sl] * (1 - xt[mT]^2) / Sqrt[cl[sl]^2 + xt[mT]^2 * sl^2];

yB0[mB_, sl_] := Sqrt[2] * mB / v * sl * cl[sl] * (1 - xb[mB]^2) / Sqrt[cl[sl]^2 + xb[mB]^2 * sl^2];

yt0[mT_, sl_] := Sqrt[2] * mt / v * 1 / Sqrt[cl[sl]^2 + xt[mT]^2 * sl^2] * (1 + df[u0]);

ytRGE =
  u / 2 * D[yt[u]^2, u] -
    yt[u]^2 / (4 * Pi)^2 *
      (9 / 2 * yt[u]^2|+ 9 / 2 * yT[u]^2 + 3 / 2 * yB[u]^2 + 1 / 4 * yM[u]^2 - 17 / 20 * g1[u]^2 -
        9 / 4 * g2[u]^2 - 8 * g3[u]^2) == 0;

yTRGE =
  u / 2 * D[yT[u]^2, u] -
    yT[u]^2 / (4 * Pi)^2 *
      (9 / 2 * yT[u]^2 + 3 / 2 * yB[u]^2 + 9 / 2 * yt[u]^2 + 1 / 4 * yM[u]^2 - 17 / 20 * g1[u]^2 -
        9 / 4 * g2[u]^2 - 8 * g3[u]^2) == 0;

yBRGE =
  u / 2 * D[yB[u]^2, u] -
    yB[u]^2 / (4 * Pi)^2 *
      (3 / 2 * yT[u]^2 + 9 / 2 * yB[u]^2 + 3 / 2 * yt[u]^2 + 1 / 4 * yM[u]^2 - 1 / 4 * g1[u]^2 -
        9 / 4 * g2[u]^2 - 8 * g3[u]^2) == 0;

yMRGE =
  u / 2 * D[yM[u]^2, u] -
    yM[u]^2 / (4 * Pi)^2 * (yT[u]^2 + yB[u]^2 + 9 / 2 * yM[u]^2 - 8 / 5 * g1[u]^2 - 8 * g3[u]^2) == 0;
```

Electroweak radiative correction term

```
xi = mH^2 / mZ^2;

A[z_] := Sqrt[Abs[1 - 4 * z]];

Z[z_] := If[z > 1 / 4, 2 * A[z] * ArcTan[1 / A[z]], A[z] * Log[(1 + A[z]) / (1 - A[z])]];

f1[M_] := 6 * Log[M^2 / mH^2] + 3 / 2 * Log[xi] - 1 / 2 * Z[1 / xi] - Z[cw / xi] - Log[cw] +
    9 / 2 * (25 / 9 - Sqrt[1 / 3] * Pi);

f0[M_] := -6 * Log[M^2 / mZ^2] * (1 + 2 * cw - 2 * mt^2 / mZ^2) + 3 * cw * xi / (xi - cw) * Log[xi / cw] +
    2 * Z[1 / xi] + 4 * cw * Z[cw / xi] + 3 * cw * Log[cw] / sw + 12 * cw * Log[cw] - 15 / 2 * (1 + 2 * cw) -
    3 * mt^2 / mZ^2 * (2 * Z[mt^2 / (mZ^2 * xi)] + 4 * Log[mt^2 / mZ^2] - 5);

fm1[M_] := 6 * Log[M^2 / mZ^2] * (1 + 2 * cw^2 - 4 * mt^4 / mZ^4) - 6 * Z[1 / xi] -
    12 * cw^2 * Z[cw / xi] - 12 * cw^2 * Log[cw] + 8 * (1 + 2 * cw^2) +
    24 * mt^4 / mZ^4 * (Log[mt^2 / mZ^2] - 2 + Z[mt^2 / (mZ^2 * xi)]);

d[M_] := Gu / Sqrt[2] * mZ^2 / (8 * Pi^2) * (xi * f1[M] + f0[M] + 1 / xi * fm1[M]);
```

Higgs sector couplings

```
lH0[mS_, sf_] := (mH^2 * cf[sf]^2 + mS^2 * sf^2) / (2 * v^2) * (1 + d[u0]);

lS0[mS_, sf_] := (mS^2 * cf[sf]^2 + mH^2 * sf^2) / (2 * w^2);

lSH0[mS_, sf_] := (mS^2 - mH^2) / (2 * w * v) * 2 * sf * cf[sf];

lHRGE =
  u / 2 * D[lH[u], u] -
    1 / (4 * Pi)^2 *
      (lH[u] * (12 * lH[u] + 6 * (yt[u])^2 + 6 * (yT[u])^2 + 6 * (yB[u])^2 - 9 / 10 * g1[u]^2 -
            9 / 2 * g2[u]^2) + 1 / 4 * lSH[u]^2 - 3 * (yt[u])^4 - 3 * (yT[u])^4 - 3 * (yB[u])^4 -
        6 * (yt[u])^2 * (yT[u])^2 + 27 / 100 * g1[u]^4 + 9 / 16 * g2[u]^4 + 9 / 40 * g1[u]^2 * g2[u]^2) ==
    0;

lSRGE =
  u / 2 * D[lS[u], u] -
    1 / (4 * Pi)^2 * (9 * lS[u]^2 + lSH[u]^2 + 6 * (yM[u])^2 * lS[u] - 6 * (yM[u])^4) == 0;

lSHRGE =
  u / 2 * D[lSH[u], u] -
    1 / (4 * Pi)^2 *
      (lSH[u] * (2 * lSH[u] + 6 * lH[u] + 3 * lS[u] + 3 * (yt[u])^2 + 3 * (yT[u])^2 +
            3 * (yB[u])^2 + 6 * (yM[u])^2 - 9 / 20 * g1[u]^2 - 9 / 4 * g2[u]^2) -
        6 * (yT[u])^2 * (yM[u])^2 - 6 * (yB[u])^2 * (yM[u])^2) == 0;

sol = ParametricNDSolve[{ytRGE, yTRGE, yBRGE, yMRGE, lHRGE, lSRGE, lSHRGE,
    yt[u0] == yt0[mT, sl], yT[u0] == yT0[mT, sl], yB[u0] == yB0[mB, sl], yM[u0] == yM0[mT, mB, sl],
    lH[u0] == lH0[mS, sf], lS[u0] == lS0[mS, sf], lSH[u0] == lSH0[mS, sf]},
   {yt, yT, yB, yM, lH, lS, lSH}, {u, u0, 10^18}, {mT, mB, mS, sl, sf}];
```

```
FixedU = 10^18;

H[mT_, mB_, mS_, sl_, sf_] := lH[mT, mB, mS, sl, sf][FixedU] /. sol

S[mT_, mB_, mS_, sl_, sf_] := lS[mT, mB, mS, sl, sf][FixedU] /. sol

SH[mT_, mB_, mS_, sl_, sf_] := lSH[mT, mB, mS, sl, sf][FixedU] /. sol

Tsp = {};
Bsp = {};
Ssp = {};
Do[SeedRandom[];
 mS = RandomReal[{300, 2200}];
 sf = RandomReal[{-1, 1}];
 mB = RandomReal[{300, 2200}];
 mT = RandomReal[{300, 2200}];
 sl = RandomReal[{-1, 1}];
 Hran = H[mT, mB, mS, sl, sf];
 Sran = S[mT, mB, mS, sl, sf];
 SHran = SH[mT, mB, mS, sl, sf];
 If[0 < Hran && 0 < Sran < 4*Pi && -4*Pi < SHran < 4*Pi, {AppendTo[Tsp, {mT, sl}];
   AppendTo[Bsp, {mB, sl}];
   AppendTo[Ssp, {mS, sf}]}, Continue[]], {3000000}]
```
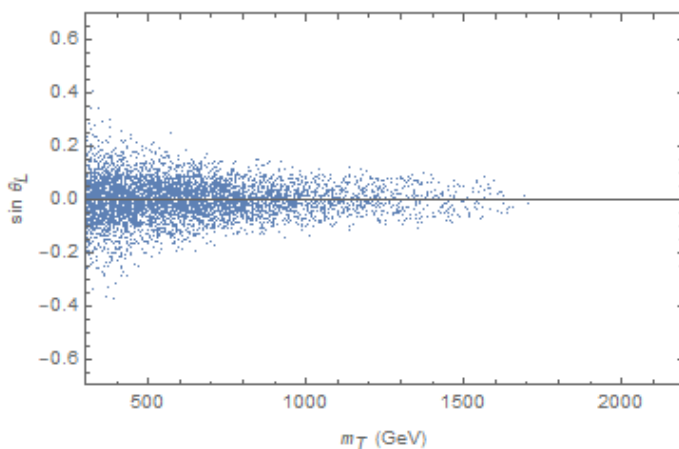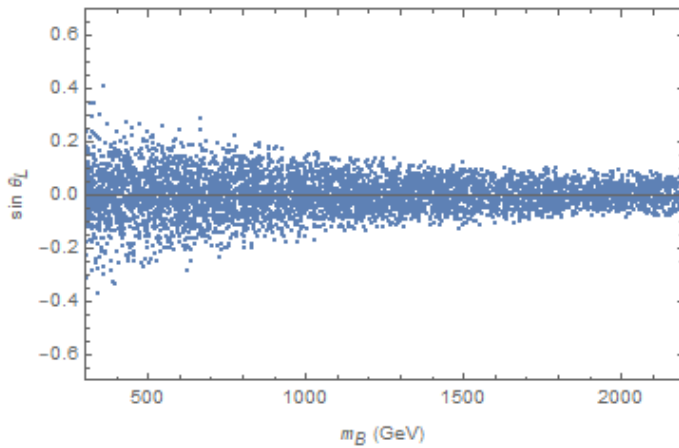
```
ListPlot[Tsp, AxesOrigin -> {300, 0}, Frame -> True, FrameLabel -> {"m_T (GeV)", "sin θ_L"},
 PlotRange -> {{300, 2200}, {-0.7, 0.7}}]
```
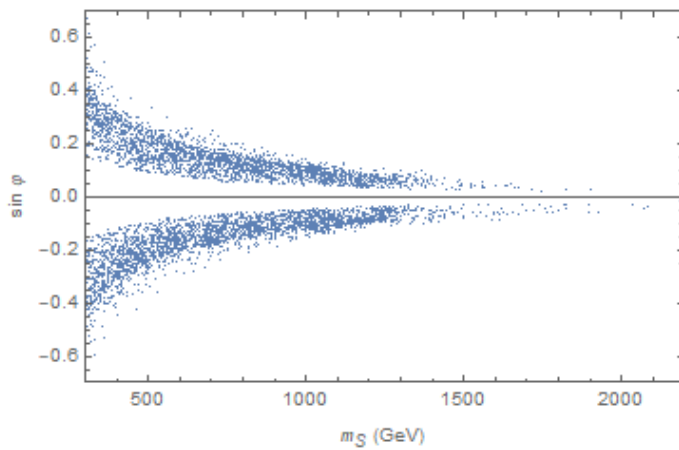
```
ListPlot[Bsp, AxesOrigin → {300, 0}, Frame → True, FrameLabel → {"m_B (GeV)", "sin θ_L"},
  PlotRange → {{300, 2200}, {-0.7, 0.7}}]
```



```
ListPlot[Ssp, AxesOrigin → {300, 0}, Frame → True, FrameLabel → {"m_S (GeV)", "sin φ"},
  PlotRange → {{300, 2200}, {-0.7, 0.7}}]
```

Bibliography

[1] Arthur H Compton. A quantum theory of the scattering of X-rays by light elements. *Physical review*, 21(5):483, 1923.

[2] Paul AM Dirac. The quantum theory of the emission and absorption of radiation. In *Proceedings of the Royal Society of London A: Mathematical, Physical and Engineering Sciences*, volume 114, pages 243–265. The Royal Society, 1927.

[3] Sheldon L Glashow. Partial-symmetries of weak interactions. *Nuclear Physics*, 22(4):579–588, 1961.

[4] Peter W Higgs. Broken symmetries and the masses of gauge bosons. *Physical Review Letters*, 13(16):508, 1964.

[5] Steven Weinberg. A model of leptons. *Physical review letters*, 19(21):1264, 1967.

[6] A Le Yaouanc, L Oliver, O Pene, and J-C Raynal. 'Naive' quark-pair-creation model of strong-interaction vertices. *Physical Review D*, 8(7):2223, 1973.

[7] Jogesh C Pati and Abdus Salam. Lepton number as the fourth 'color'. *Physical Review D*, 10(1):275, 1974.

[8] CMS collaboration et al. Observation of a new boson at a mass of 125 GeV with the CMS experiment at the LHC. *arXiv preprint arXiv:1207.7235*, 2012.

[9] Georges Aad, T Abajyan, B Abbott, J Abdallah, S Abdel Khalek, AA Abdelalim, O Abdinov, R Aben, B Abi, M Abolins, et al. Observation of a new particle in the search for the Standard Model Higgs boson with the ATLAS detector at the LHC. *Physics Letters B*, 716(1):1–29, 2012.

[10] Marc Sher. Precise vacuum stability bound in the standard model. *Physics Letters B*, 317(1-2):159–163, 1993.

[11] Dario Buttazzo, Giuseppe Degrassi, Pier Paolo Giardino, Gian F Giudice, Filippo Sala, Alberto Salvio, and Alessandro Strumia. Investigating the near-criticality of the Higgs boson. *Journal of High Energy Physics*, 2013(12):1–49, 2013.

[12] Jose R Espinosa. Implications of the top (and Higgs) mass for vacuum stability. *arXiv preprint arXiv:1512.01222*, 2015.

[13] Mariana Frank and Subhadeep Mondal. Light neutralino dark matter in U(1)âĂš models. *Physical Review D*, 90(7):075013, 2014.

[14] Durmuş Ali Demir, Mariana Frank, and Beste Korutlu. Dark matter from conformal sectors. *Physics Letters B*, 728:393–399, 2014.

[15] Matthew Gonderinger, Hyungjun Lim, and Michael J Ramsey-Musolf. Complex scalar singlet dark matter: vacuum stability and phenomenology. *Physical Review D*, 86(4):043511, 2012.

[16] Seungwon Baek, P Ko, Wan-Il Park, and Eibun Senaha. Vacuum structure and stability of a singlet fermion dark matter model with a singlet scalar messenger. *JHEP*, 11(11):6, 2012.

[17] Valentin V Khoze, Christopher McCabe, and Gunnar Ro. Higgs vacuum stability from the dark matter portal. *arXiv preprint arXiv:1403.4953*, 2014.

[18] J Velhinho, R Santos, and A Barroso. Tree level vacuum stability in two-Higgs-doublet models. *Physics Letters B*, 322(3):213–218, 1994.

[19] Fatemeh Arbabifar, Sahar Bahrami, and Mariana Frank. Neutral Higgs bosons in the Higgs triplet model with nontrivial mixing. *Physical Review D*, 87(1):015020, 2013.

[20] Sahar Bahrami and Mariana Frank. Vector leptons in the higgs triplet model. *Physical Review D*, 88(9):095002, 2013.

[21] Shankha Banerjee, Mariana Frank, and Santosh Kumar Rai. Higgs data confronts sequential fourth generation fermions in the Higgs triplet model. *Physical Review D*, 89(7):075005, 2014.

[22] Sahar Bahrami and Mariana Frank. Dark matter in the Higgs triplet model. *Physical Review D*, 91(7):075003, 2015.

[23] Ming-Lei Xiao and Jiang-Hao Yu. Stabilizing electroweak vacuum in a vectorlike fermion model. *Physical Review D*, 90(1):014007, 2014.

[24] Jue Zhang and Shun Zhou. Electroweak vacuum stability and diphoton excess at 750 GeV. *Chinese Physics C*, 40(8):081001, 2016.

[25] Priyotosh Bandyopadhyay and Rusa Mandal. Vacuum stability in extended standard model with leptoquark. *arXiv preprint arXiv:1609.03561*, 2016.

[26] Keith R Dienes, Emilian Dudas, and Tony Gherghetta. Light neutrinos without heavy mass scales: a higher-dimensional seesaw mechanism. *Nuclear Physics B*, 557(1-2):25–59, 1999.

[27] Ernest Ma. Verifiable radiative seesaw mechanism of neutrino mass and dark matter. *Physical Review D*, 73(7):077301, 2006.

[28] Satoshi Iso, Nobuchika Okada, and Yuta Orikasa. Classically conformal B–L extended Standard Model. *Physics Letters B*, 676(1):81–87, 2009.

[29] D. Griffiths. *Introduction to Elementary Particles.* John Wiley & Sons, New York, USA, 1987.

[30] Giovanni Organtini. Unveiling the higgs mechanism to students. *European Journal of Physics*, 33(5):1397, 2012.

[31] Summary of the Standard Model. `http://bolvan.ph.utexas.edu/~vadim/classes/11f/SM.pdf`. Accessed: 2017-05-03.

[32] Marie E Machacek and Michael T Vaughn. Two-loop renormalization group equations in a general quantum field theory:(i). Wave function renormalization. *Nuclear Physics B*, 222(1):83–103, 1983.

[33] Marie E Machacek and Michael T Vaughn. Two-loop renormalization group equations in a general quantum field theory (ii). Yukawa couplings. *Nuclear Physics B*, 236(1):221–232, 1984.

[34] Marie E Machacek and Michael T Vaughn. Two-loop renormalization group equations in a general quantum field theory:(iii). Scalar quartic couplings. *Nuclear Physics B*, 249(1):70–92, 1985.

[35] Lee Smolin. *Three roads to quantum gravity.* Basic Books, 2002.

[36] Gianfranco Bertone, Dan Hooper, and Joseph Silk. Particle dark matter: Evidence, candidates and constraints. *Physics Reports*, 405(5):279–390, 2005.

[37] Alexander Alexandrovich Antonov. Hidden Multiverse: explanation of dark matter and dark energy. *Journal of Cosmology*, 2015.

[38] Laurent Canetti, Marco Drewes, and Mikhail Shaposhnikov. Matter and antimatter in the universe. *New Journal of Physics*, 14(9):095012, 2012.

[39] James H Christenson, Jeremiah W Cronin, Val L Fitch, and René Turlay. Evidence for the 2π decay of the K 2 0 meson. *Physical Review Letters*, 13(4):138, 1964.

[40] R Aaij, C Abellan Beteta, B Adeva, M Adinolfi, C Adrover, A Affolder, Z Ajaltouni, J Albrecht, F Alessio, M Alexander, et al. First observation of CP violation in the decays of Bs (0) mesons. *Physical review letters*, 110(22):221601, 2013.

[41] JP Lees, V Poireau, V Tisserand, J Garra Tico, E Grauges, A Palano, G Eigen, B Stugu, DN Brown, LT Kerth, et al. Observation of time-reversal violation in the B-0 meson system. *Physical review letters*, 109(21):211801, 2012.

[42] Guido Altarelli and Gino Isidori. Lower limit on the Higgs mass in the standard model: An Update. *Physics Letters B*, 337(1):141–144, 1994.

[43] Yong Tang. Vacuum stability in the standard model. *Modern Physics Letters A*, 28(04):1330002, 2013.

[44] A Sirlin and R Zucchini. Dependence of the Higgs coupling hMS (M) on mH and the possible onset of new physics. *Nuclear Physics B*, 266(2):389–409, 1986.

[45] Ralf Hempfling and Bernd A Kniehl. Relation between the fermion pole mass and MS⁻ Yukawa coupling in the standard model. *Physical Review D*, 51(3):1386, 1995.

[46] Shrihari Gopalakrishna, Tanumoy Mandal, Subhadip Mitra, and Grégory Moreau. LHC signatures of warped-space vectorlike quarks. *Journal of High Energy Physics*, 2014(8):79, 2014.

[47] Tao Han, Heather E Logan, Bob McElrath, and Lian-Tao Wang. Phenomenology of the little Higgs model. *Physical Review D*, 67(9):095004, 2003.

[48] Tim Pieter Tjipko Dijkstra, LR Huiszoon, and Adrian Norbert Schellekens. Supersymmetric standard model spectra from RCFT orientifolds. *Nuclear Physics B*, 710(1):3–57, 2005.

[49] Roberto Contino, Leandro Da Rold, and Alex Pomarol. Light custodians in natural composite Higgs models. *Physical Review D*, 75(5):055014, 2007.

[50] Nicolas Bonne and Gregory Moreau. Reproducing the Higgs boson data with vector-like quarks. *Physics Letters B*, 717(4):409–419, 2012.

[51] Dean Carmi, Adam Falkowski, Eric Kuflik, and Tomer Volansky. Interpreting LHC Higgs results from natural new physics perspective. *Journal of High Energy Physics*, 2012(7):136, 2012.

[52] Sebastian AR Ellis, Rohini M Godbole, Shrihari Gopalakrishna, and James D Wells. Survey of vector-like fermion extensions of the Standard Model and their phenomenological implications. *Journal of High Energy Physics*, 2014(9):130, 2014.

[53] Juan Antonio Aguilar-Saavedra, Rachid Benbrik, Sven Heinemeyer, and Manuel Pérez-Victoria. Handbook of vectorlike quarks: Mixing and single production. *Physical Review D*, 88(9):094010, 2013.

[54] G Moreau. Constraining extra fermion(s) from the Higgs boson data. *Physical Review D*, 87(1):015027, 2013.

[55] John F Gunion. Extended Higgs sectors. *arXiv preprint hep-ph/0212150*, 2002.

[56] Ling-Fong Li and Feng Wu. Coupling constant unification in extensions of standard model. *International Journal of Modern Physics A*, 19(19):3217–3224, 2004.

[57] JA Aguilar-Saavedra. Effects of mixing with quark singlets. *Physical Review D*, 67(3):035003, 2003.